LBL-12965
Preprint

Lawrence Berkeley Laboratory
UNIVERSITY OF CALIFORNIA

Materials & Molecular Research Division

RECEIVED
LAWRENCE
BERKELEY LABORATORY
JAN 14 1982
LIBRARY AND
DOCUMENTS SECTION

Submitted to Electrochimica Acta

NUCLEATION AND GROWTH OF ANODIC SILVER OXIDE FILMS:
LIGHT SCATTERING & ELLIPSOMETER MEASUREMENTS

R.H. Muller, W.J. Plieth, and J.C. Farmer

November 1981

TWO-WEEK LOAN COPY

This is a Library Circulating Copy
which may be borrowed for two weeks.
For a personal retention copy, call
Tech. Info. Division, Ext. 6782

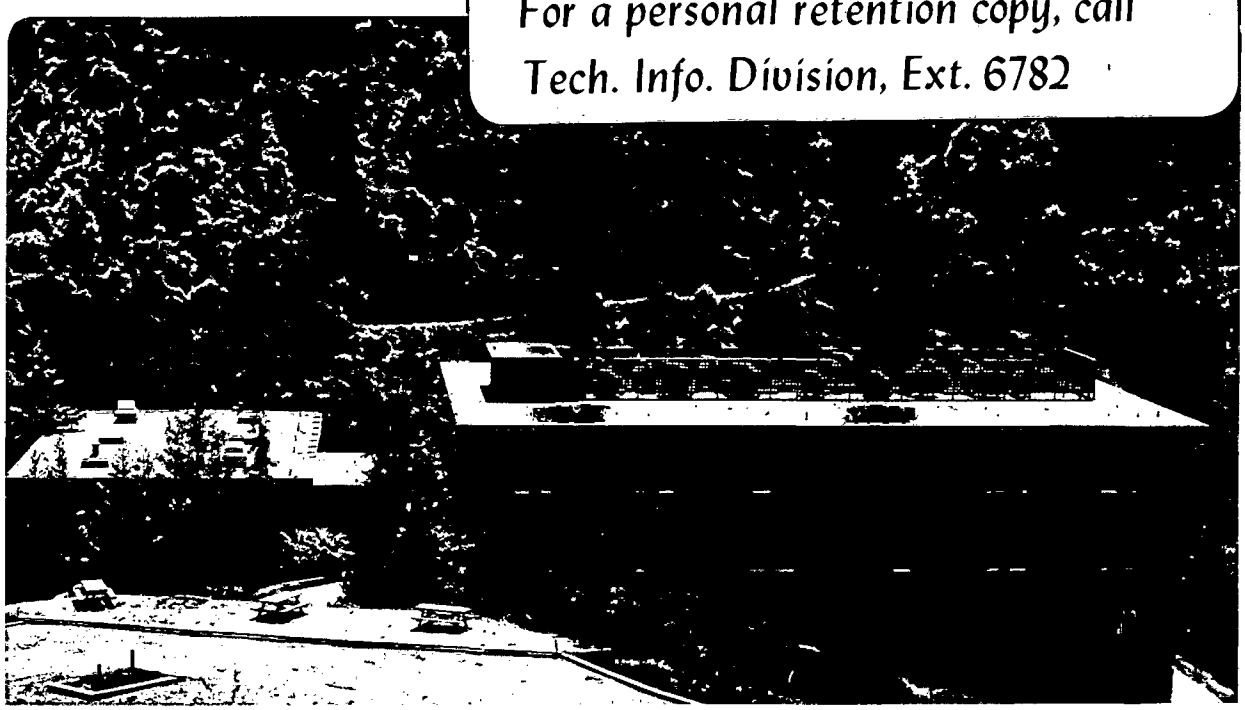

Prepared for the U.S. Department of Energy under Contract W-7405-ENG-48

LBL-12965 c.2

DISCLAIMER

This document was prepared as an account of work sponsored by the United States Government. While this document is believed to contain correct information, neither the United States Government nor any agency thereof, nor the Regents of the University of California, nor any of their employees, makes any warranty, express or implied, or assumes any legal responsibility for the accuracy, completeness, or usefulness of any information, apparatus, product, or process disclosed, or represents that its use would not infringe privately owned rights. Reference herein to any specific commercial product, process, or service by its trade name, trademark, manufacturer, or otherwise, does not necessarily constitute or imply its endorsement, recommendation, or favoring by the United States Government or any agency thereof, or the Regents of the University of California. The views and opinions of authors expressed herein do not necessarily state or reflect those of the United States Government or any agency thereof or the Regents of the University of California.

NUCLEATION AND GROWTH OF ANODIC SILVER OXIDE FILMS: LIGHT SCATTERING & ELLIPSOMETER MEASUREMENTS

R. H. Muller, W. J. Plieth*, and J. C. Farmer

Materials and Molecular Research Division
Lawrence Berkeley Laboratory
University of California
Berkeley, CA 94720

ABSTRACT

During the initial phase of the formation of Ag_2O on Ag in KOH, the onset of light scattering coincides with the rapid change in ellipsometer measurements. Nucleation of the oxide phase, as indicated by a maximum in overpotential, precedes the rise of light scattering.

*Permanent address: Institut fur Physikalische Chemie, Freie Universitat Berlin, Takustrasse 3, 1000 Berlin 33.

INTRODUCTION

The formation of anodic oxide layers on silver had been interpreted previously[1] as involving several successive processes that include the nucleation and growth of particulate films. Since particle size was found to be well below the wavelength of light, the effect of particles was represented by optically equivalent films for the interpretation of the ellipsometer measurements. Even such small particles can, however, result in measurable light scattering and this work was undertaken to compare scattering and ellipsometer measurements.

EXPERIMENTAL

The electrode consisted of a high-purity silver sheet (0.5 x 5 x 0.2 cm 60% immersed in the electrolyte). It was located in a cylindrical glass cell of 4 cm diameter and illuminated with the beam from an argon ion laser (wavelength 514.5 nm, power of 30 mW) at an angle of incidence (measured from the surface normal) of 60° or 75°. A platinum gauze in the lower part of the cell served as counter electrode and mercuric oxide was used for the reference electrode. The tip of its Luggin capillary was located 1 cm from the back side of the electrode (which was also active). The electrode surface was polished mechanically with 0.05 μm Al_2O_3 paste and chemically with a 1ℓ solution containing 24g CrO_3 and 20 ml HCl(24%). The electrolyte (1.0 M KOH) was prepared with distilled water and analytical grade KOH pellets. All optical measurements were performed during galvanostatic polarization at 0.3 $\frac{mA}{cm^2}$. Cyclic voltammetry was also used.

Dynamic values of the ellipsometer parameters ψ and Δ were measured by the same automatic ellipsometer used for earlier studies of anodic oxide films on silver.[1] However, the instrument had been modified by the use of an argon ion laser (Lexel Model 75) as a light source and a microcomputer (LSI-11) for data acquisition. The laser is essential for scattering experiments with rough surfaces.

Scattered light was collected with a fiber-optics probe of about 1 mm diameter which was rotated in the plane of incidence around the electrode at a distance of 6 cm. A photomultiplier (RCA R136, operated at voltages around 1000V) served as light detector.

The microcomputer simultaneously monitored the cell current, cell potential, ellipsometer parameters, and the scattered light intensity. Data were digitally filtered by averaging 30 points per half second for each channel.

Scanning electron micrographs were obtained of several electrode surfaces after current interruption at time intervals characteristic of the different stages of light scattering from the surface. Electrodes were removed from solution, rinsed with distilled water, coated with a thin layer of gold to improve SEM resolution, and then placed in the SEM (AMR 1000). The gold was plasma deposited for 2-1/2 minutes at 20 mA in a 0.04 Torr argon atmosphere. Magnifications of 5, 10, and 20 x 10^5 were used, with a beam energy of 30 keV.

RESULTS AND DISCUSSION

1.) Light Scattering Data

The time-dependence of light-scattering measurements (Fig. 1) is characterized by an initial period during which no change is detected, followed by a linear increase in intensity. Eventually the measured scattering intensity passes through a maximum.

The dependence of the scattering intensity on scattering angle (measured from the direction of the specularly reflected beam) is shown in Fig. 2. Scattering is peaked in the forward direction and increases with increasing charge passed through the electrode.

By use of the two linear parts of the light scattering curve, an induction time can be defined, as shown in Fig. 1. The slope of the rising portion of the scattering curve depends on current density, as shown in Fig. 3. Over the small spectral range accessible with the argon

ion laser (458-514 mm), the induction time, as defined in Fig. 1, did not vary with wavelength (Fig. 4). Induction time was also independent of scattering angle (Fig. 5).

Scattering from rough surfaces and its effect on ellipsometry have been discussed before.[2-5] Although theories exist regarding rough surface effects on the state of polarization of reflected and scattered light,[6-11] they do not account quantitatively for observations.

One expects that as the number of surface irregularities increases scattering from the surface also increases, and that as the size of these irregularities become of the same magnitude as the wavelength of light, their effectiveness as scattering centers is enhanced.

It has been shown[6,7] that the scattered light intensity, I_s, is proportional to the square of the ratio of the rms deviation of surface roughness, δ, to the wavelength, λ of incident light

$$\frac{I_s}{I_i} \propto \delta^2 \left(\frac{\omega}{c}\right)^2 \propto \left(\frac{\delta}{\lambda}\right)^2 \qquad \text{for } \delta<\lambda$$

where ω and c are the frequency and vacuum velocity of light.

As the particles continue to grow, the light scattering power of the surface reaches some limit. If the particles are visualized as perfectly round spheres sitting on a plane, both the particle diameter and the apparent surface coverage are limited as the particles become close packed.

As the particles become larger and grow closer together, a fraction of the incident light is absorbed by multiple scattering and light trapping.

2.) Simultaneous Ellipsometer-Scattering Data

The onset of light scattering, shown in Fig. 6 at 5 sec, coincides with the rapid change in the ellipsometer parameter Δ, shown for the same conditions in Fig. 7, and that of the parameter ψ, shown in Fig. 8. It can be seen that changes in surface properties are detected by the ellipsometry before scattering is measurable.

A peak in the measured electrode potential, shown at 3 sec in Fig. 9, indicates the nucleation of the oxide phase and its growth from a supersaturated solution and confirms the previous interpretation.[1] A growth of the nuclei has to take place before they cause light scattering. Even after a short period of growth, the oxide particles are stable in the electrolyte under open circuit conditions, as shown in Fig. 10. The scattering phenomenon results in a discontinuity in the ψ-Δ plot shown in Fig. 11.

3. SEM Data

Figures 12 through 15 are electron micrographs of electrode surfaces at different stages of particle growth and light scattering. These photographs correspond to points (a) through (d) on Fig. 1, respectively. The photographs are quantified in Table I. Figure 12 represents the surface before the onset of light scattering. The particle shown in the picture is an extraneous dust particle used to focus the instrument. No Ag_2O particles were found on this electrode large enough to be seen by the SEM (<200Å). The charge passed was 9.0×10^{-4} coulombs/cm^2. Ellipsometry parameters at this stage are close to initial values (Δ=45° and ψ=36°). Based upon the charge passed, assuming 100% current efficiency, and formation of a non-porous film of bulk density, one computes an oxide film thickness of 15Å.

Figure 13 is taken immediately after the onset of light scattering (Point b, Fig. 1). Unfortunately, this electrode was not as highly polished as other specimens, so the roughness factor is greater. The approximate number density of Ag_2O particles on this electrode is 1.7 x 10^9 cm^{-2} with all of the particles falling below 5000Å. The largest particle in this photograph is 2000Å, but more typically particles are about 1000Å. The particle dimensions from SEM photographs (1000Å) are consistent with an expected particle size (786Å) computed by distributing the amount of oxide formed, assuming 100% current efficiency, into nonporous spherical particles with the observed number density. At this stage of development, the scattering intensity is about 14% of its maximum (taking the initial intensity as a zero baseline) and the ellipsometer parameter Δ changes very fast (about 25°/sec, change of 20° overall).

Figure 14 is taken at the point of maximum scattering intensity (100%) (Point c, Fig. 1). The smoothness of the original surface is comparable to that of Fig. 12, and the number density of particles on this surface is about 0.7 x 10^9 cm^{-2}.

The largest particle in the photograph is 2500Å, with typical sizes being 1500Å. Based upon number density and charge passed, a particle size of 1500Å is computed. Changes in Δ and ψ are more gradual after the initial nucleation and growth of particles on the surface. Changes in number density between points (a) through (c) of Fig. 1 are not clear, but it is evident that the particle formation coincides with both increased light scattering and rapid change in Δ, and that after particles are formed, they grow in size. The greater number density at point (b)

compared to point (c) may be attributable to the different roughness of the original surface.

Scattering intensity-time curves are all characterized by a maximum which is followed by a gradual decrease. At point (d) the scattering intensity is only 64% of the maximum (c). The number density of particles on this surface (Fig. 15) is about 0.8×10^8 cm^{-2}, with only 35% of the particles falling below 5000Å. The largest particle in the photograph is 6000Å, with typical values being 5000Å. Based upon number density and charge passed, a particle size of 3300Å is computed, the discrepancy is probably due to the irregular shape of the particles. Ag_2O distributed in a uniform, compact film, results in a thickness of 421Å. Values of Δ and ψ continue to change gradually. It is interesting that in this photograph, the number density of particles is the same as that for Fig. 14. The substrate roughness from electrode preparation for both of these specimens are comparable. Particles are therefore nucleated at the same time and grow continuously afterwards. The decrease in scattering intensity appears to be related to the size of the particles with scattering efficiency decreasing as particle size exceeds the wavelength of the incident light.

4.) Applicability of Ellipsometry Models

The film thickness values computed from the charge passed and assuming a compact layer of Ag_2O were used to calculate values of Δ and ψ and the results are given in Table II. Clearly, this model is inadequate since the errors in Δ after the onset of scattering are as great as 23° at the maximum scattering intensity. Errors in ψ are substantially less than those in Δ. The errors in Δ are correlated with the

measured scattering intensity, i.e., the greater the scattering, the greater the error in Δ.

Attempts were also made to use the coherent superposition model[1] and the Bruggeman effective media approximation[2] to explain the ellipsometry data. The results are summarized in Tables III and IV. Both of these models were capable of fitting the data, unlike the simple film model. This is due to the two available adjustable parameters, the apparent film thickness, T, and the apparent surface coverage θ. The simple homogeneous film model has only one adjustable parameter, T.

The coherent superposition model visualizes the surface as a bare substrate, covered with islands of silver oxide film. The fraction of the surface covered by islands is θ, the thickness of each island being T. In this case, one takes a weighted average of the Fresnel reflection coefficients for the bare and film covered surface.

$$r_\nu = \theta r_{\nu f} + (1-\theta) r_{\nu e} \qquad \nu = s,p \tag{1}$$

Here, f and e denote the film and electrode substrate, and s and p are the respective polarizations. The relative phase and amplitude, Δ and ψ, are then computed using this weighted average. To fit the data minima are found in the sum-of-squares surface, S. Values of T and θ at the minima are denoted with a subscript "c".

$$S = |S\Delta^\circ|^2 + |S\psi^\circ|^2 \tag{2.a}$$

$$S\Delta^\circ = \Delta_m{}^\circ - \Delta_c{}^\circ \tag{2.b}$$

$$S\psi^\circ = \psi_m{}^\circ - \psi_c{}^\circ \tag{2.c}$$

where Δ°_m and $\psi^\circ m$ are measured elipsometer parameters, and $\Delta_c{}^\circ$ and $\psi_c{}^\circ$ are model predictions. In seeking fits of the experimental data, the coherent superposition model yields two solutions for particle-covered surfaces. Both solutions are given in Table III. Both parameters T_c and θ_c, are of the same magnitude as the particle diameters, D_{SEM}, and the surface coverage, θ_{SEM}, as determined by the scanning electron microscope. Qualitatively, trends are the same as well. In the table, θ_{SEM} was calculated from the particle diameter, D_{SEM}, and the number density on the surface, N_{SEM}.

$$\theta_{SEM} = N_{SEM} \frac{\pi}{4} D_{SEM}{}^2 \tag{3}$$

The Bruggeman model is different from the coherent superposition model in that one now takes a weighted average of the dielectric constants (complex) for the silver oxide, $\hat{\varepsilon}_f$, and for the electrolyte, $\hat{\varepsilon}_o$, to determine an apparent film dielectric constant, $\hat{\varepsilon}_h$. The complex dielectric constant, $\hat{\varepsilon}_h$ is then used to calculate the complex refractive index of the film. This refractive index is then used to predict Δ and ψ at different film thicknesses.

$$\theta \frac{\hat{\varepsilon}_f - \hat{\varepsilon}_h}{\hat{\varepsilon}_f + 2\hat{\varepsilon}_h} + (1-\theta) \frac{\hat{\varepsilon}_o - \hat{\varepsilon}_h}{\hat{\varepsilon}_o + 2\hat{\varepsilon}_h} = 0 \tag{4}$$

Given θ, $\hat{\varepsilon}_f$, and $\hat{\varepsilon}_o$, this equation is easily solved for $\hat{\varepsilon}_h$. Here, the refractive index is varied directly by the apparent surface coverage. Unlike the coherent superposition model, the Bruggeman approach yields only one actual solution, but has two deep minima in the S surface. Both minima (one being the solution) are given

in Table IV. Again, T_c and θ are of the same magnitudes as D_{SEM} and θ_{SEM}, respectively. One minimum (not the "best fit") corresponds to a simple homogeneous film (θ=1); however, the composite error $S^{1/2}$ is quite large compared to that for the solution; a single adjustable parameter is inadequate to explain the ellipsometry data.

Calculations based on both the coherent superposition model and the Bruggeman approximation did not vary the values of the substrate refractive index or the refractive indices of the silver oxide and electrolyte. The substrate refractive index was determined from ellipsometer measurements at time zero, before any current was passed. Approximate values of the silver oxide and electrolyte refractive indices were taken from reference 1. Computer programs and example output are given in the appendices and were written for the LSI-11 Fortran compiler.

CONCLUSIONS

The present study supports the previous multi-dimensional interpretation of ellipsometer measurements in which an oxidation mechanism involving nucleation and growth of oxide particles via a dissolution-precipitation mechanism had been proposed. The particles discussed here represent the primary layer of the model and are much smaller than the secondary crystals shown previously, which had formed after much longer times.

The onset of light scattering from the surface occurs a short time after particle nucleation, and is accompanied by a corresponding rapid change in the relative phase Δ as determined by the ellipsometer.

After reaching a maximum level, the scattering intensity begins to decrease. At the maximum, the particle size is less than the wavelength of the incident light, whereas after the decrease in scattering intensity, the particles exceed the dimension of the wavelength of incident light. The existence of this maximum could be due to a shift in scattering regime or light trapping between the more closely spaced, larger particles.

Scanning electron micrographs of the electrode surface (after current interruption at various stages of particle growth) seem to indicate that the number density of particles on the surface does not increase with time, but remains relatively constant. However, the particles grow in size. Thus, the nucleation of these particles seems to occur at the same instant (one-time nucleation) after which particle growth only occurs. Thus the increase in scattering intensity has to be due to particle growth, and not the formation of additional particles.

A simple, single parameter film model is inadequate to describe the discontinuity in the ellipsometer data. However, either the Bruggeman effective media or the coherent superposition model can qualitatively explain trends in the ellipsometry data. The model predictions of the film thickness T_c and apparent surface coverage θ_c agree approximately with the range of particle diameters and surface coverages, D_{SEM} and θ_{SEM}, as determined from electron micrographs.

ACKNOWLEDGMENTS

This work was supported in part by the Director, Office of Energy Research, Office of Basic Energy Sciences, Materials Sciences Division of the U.S. Department of Energy under contract No. W-7405-ENG-48. We also wish to thank the Deutsche Forschengsgemeinschaft for the support of one author (W.J.P.).

REFERENCES

1. Muller, R. H., Smith, C. G., Surf. Sci. 96, 375 (1980).
2. Aspnes, D. E., Theeten, J. B., Hottier, F., Phys. Rev. B 20, 3292 (1979).
3. Smith, T., Surf. Sci. 56, 252 (1976).
4. Ohlidal, I., Lukes, F., Navratil, K., Surf. Sci. 45, 91 (1974).
5. Azzam, R. M. A., Bashara, N. M., Phys. Rev. B 5, 4721 (1972).
6. Marvin, A., Toigo, R., Celli, V., Phys. Rev. B 11, 2777 (1975).
7. Celli, V., Marvin, A., Phys. Rev. B 11, 1779 (1975).
8. Maradudin, A. A., Mills, D. L., Phys. Rev. B 11, 1392 (1975).
9. Sichel, E. K., Gittleman, J. I., Abeles, B., Thin Solid Films 51, 89 (1978).
10. Ohlidal, I., Lukes, F., Opt. Acta 19, 817 (1972).
11. Berreman, D. W., J. Opt. Soc. Am. 60, 499 (1970).

Table I. Evaluation of SEM Photographs.

Micrograph Point on Fig. 1		Fig. 12 a	Fig. 13 b*	Fig. 14 c	Fig. 15 d
TIME (s)		3	8	24	84
CURRENT DENSITY (mA/cm^2)		0.3	0.3	0.3	0.3
CHARGE PASSED ($coulombs/cm^2$)		9.0×10^{-4}	2.4×10^{-3}	7.1×10^{-3}	2.5×10^{-2}
NUMBER DENSITY OF PARTICLES ON SURFACE	(cm^{-2})	0	1.66×10^{9}	0.71×10^{9}	0.75×10^{9}
% BELOW 5000 Å	(%)	100	100	100	35
% ABOVE 5000 Å	(%)	0	0	0	65
LARGEST PARTICLE SIZE	(Å)	<200	2000	2500	6000
TYPICAL PARTICLE SIZE	(Å)	-	1000	1500	5000
EXPECTED PARTICLE SIZE**	(Å)	-	786	1500	3300
EXPECTED COMPACT FILM THICKNESS	(Å)	15	41	120	421
TYPICAL VALUE OF Δ (deg)		45	25	15	-5
TYPICAL VALUE OF ψ (deg)		36	36	39	46
SCATTERING INTENSITY (% of maximum)		~0	~14	100	64

*Unusually high surface roughness from electrode polishing.
**Based on number density and charge balance.

Table II. Inability of Simple Film Model to Account for Observed Values of Δ and ψ Assuming Homogeneous Compact Ag_2O Layer.

assumed optical properties $n_o = 1.34$

$\hat{n}_f = 2.17 - 0.28\ i$

$\hat{n}_s = 1.01 - 1.58\ i$

t(s)	d(A)	Δ°_m	Δ°_c	$\lvert\delta\Delta^\circ\rvert$	ψ°_m	ψ°_c	$\lvert\delta\psi^\circ\rvert$
0	0	45.00	45.00	0	36.75	36.75	0
3	15	45	43.92	1°	36	36.98	1°
8	41	25	42.10	17°	36	37.42	1°
24	120	15	37.49	23°	39	39.23	<1°
84	421	- 5	- 12.04	7°	46	50.60	5°

Note: n_o and $\hat{n}_f$ were taken from reference 1 as approximate values and n_s was measured by the ellipsometer. Here t is time, d the computed compact film thickness based on the charge balance; m and c denote measured and calculated parameters, respectively; s denotes an error value.

Table III. Effective Film Thickness and Coverage Predicted by Coherent Superposition Model Compared to SEM Data.

assumed optical properties $n_o = 1.34$

$\hat{n}_f = 2.17 - 0.28\ i\ (\theta=1)$

$\hat{n}_s = 1.01 - 1.58\ i$

t(s)	Δ°_m	Δ°_c	ψ°_m	ψ°_c	$\lvert S\Delta^\circ\rvert^2 + \lvert S\psi^\circ\rvert^{1/2}$	T_c(A)	θ_c	D_{SEM}(A)	θ_{SEM}
0	45.00	45.00	36.75	36.75	0.00	0	0	0	0
3	45	45.00	36	36.76	0.76	0	0	0	0
8	25	24.93	36	35.99	0.07	710	0.32	786-2000	0.09-0.52
		25.05	-	36.08	0.09	1560	0.72		
24	15	14.88	39	39.04	0.13	580	0.47	1500-2500	0.13-0.35
		15.13		38.93	0.15	1750	0.76		
84	- 5	- 4.69	46	46.26	0.40	480	0.80	3300-6000	0.64-1.00
		- 4.16		46.44	0.95	2880	0.62		

Note: Through minimization of the sum of squares surface for ψ and Δ, two possible values of T_c and θ_c were found; i.e., multiple solutions.

Table IV. Effective Film Thickness and Coverage predicted by Bruggeman Effective Media Approximation Model Compared to SEM Data.

assumed optical properties $n_o = 1.34$

$\hat{n}_f = 2.17 - 0.28\ i\ (\theta=1)$

$\hat{n}_s = 1.01 - 1.58\ i$

t(s)	Δ°_m	Δ°_c	ψ°_m	ψ°_c	$\left[\lvert S\Delta^\circ\rvert^2 + \lvert S\psi^\circ\rvert^2\right]^{1/2}$	T_c(A)	θ_c	D_{SEM}(A)	θ_{SEM}
0	45.00	45.00	36.75	36.75	0.00	0	0	0	0
3	45	45.03	36	35.97	0.04	0	0	0	0
8	25	25.07	36	36.03	0.07	2310	0.52	786-2000	0.09-0.52
		31.20		44.28	10.35	240	1		
24	15	15.17	39	39.02	0.17	2370	0.59	1500-2500	0.13-0.35
		18.98		50.36	12.03	330	1		
84	-5	-5.10	46	45.86	0.17	3250	0.42	3300-6000	0.64-1.00
		-6.69		52.97	7.18	420	1		

Note: Although there is only one solution per data point, two deep minima exist in the sum of squares for the 8, 24, and 84 second data points. One minima corresponds to a compact film model.

FIGURE CAPTIONS

Fig. 1. Time-dependance of the intensity of scattered light (shown as photomultiplier current) during the anodic formation of Ag_2O in 1.0 MKOH, 0.4 mA/cm^2 and locus of micrographs shown in Figs. 12-15. Angle of incidence for incident beam 75°, scattering angle 30° from specular beam.

Fig. 2. Dependance of light scattering on scattering angle (measured from specularly reflected beam) for different amounts of charge passed, 0.2 mA/cm^2.

Fig. 3. Slope of linear part of light scattering curve for different current densities. Scattering angle 20°.

Fig. 4. Induction time as defined in Fig. 8 for different wavelengths. 0.20 mA/cm^2, 10 sec, scattering angle 12°.

Fig. 5. Induction time as defined in Fig. 8 for different scattering angles.

Fig. 6. Intensity of scattered light during film formation 1.2 MKOH, 0.2 mA/cm^2, angle of incidence 75°, scattering angle 55°.

Fig. 7. Measured ellipsometer parameter Δ under same conditions as in Fig. 6.

Fig. 8. Measured ellipsometer parameter ψ under same conditions as in Fig. 6.

Fig. 9. Electrode potential measured under the conditions of Fig. 6.

Fig. 10. Particle stability determined from scattering intensity at 0.2 mA/cm^2 and scattering angle 20°.

Fig. 11. Measured ellipsometer parameters Δ and ψ and scattered light intensities measured at 60° scattering angle. Film growth proceeds from lower right to upper left. Summary of measurement 0.2 to 0.5 mA/cm^2. The numbers given on the figure are scattering intensities normalized by the measured level at the beginning of the experiment.

Fig. 12. Scanning electron micrograph of silver electrode surface before onset of light scattering, 0.2 mA/cm^2, 3 sec (Fig. 1, point a). Magnification of 20 x 10^3 X.

Fig. 13. Electrode surface at onset of light scattering, 0.2 mA/cm^2, 8 sec (Fig. 1, point b). Magnification of 20 x 10^3 X.

Fig. 14. (a&b) Electrode surface near peak of light scattering, 0.2 mA/cm^2, 24 sec (Fig. 1, point c). Magnification of 20 x 10^3 X, and 10^4 X, respectively.

Fig. 15. (a&b) Electrode surface after decrease of light scattering, 0.2 mA/cm^2, 84 sec (Fig. 1, point d). Magnifications of 20 x 10^3 X, and 10^4 X, respectively.

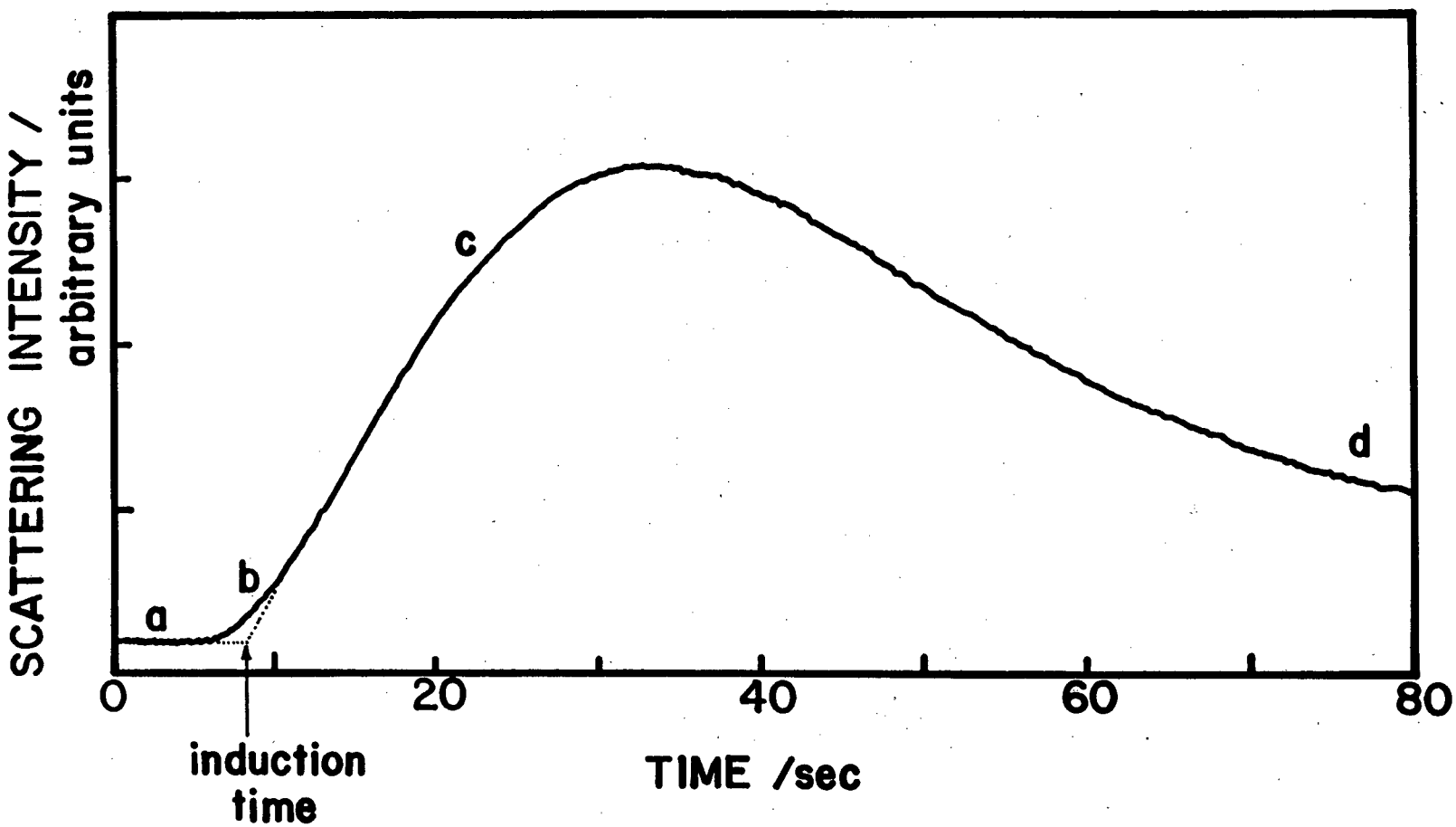

XBL 817-10529

Fig. 1

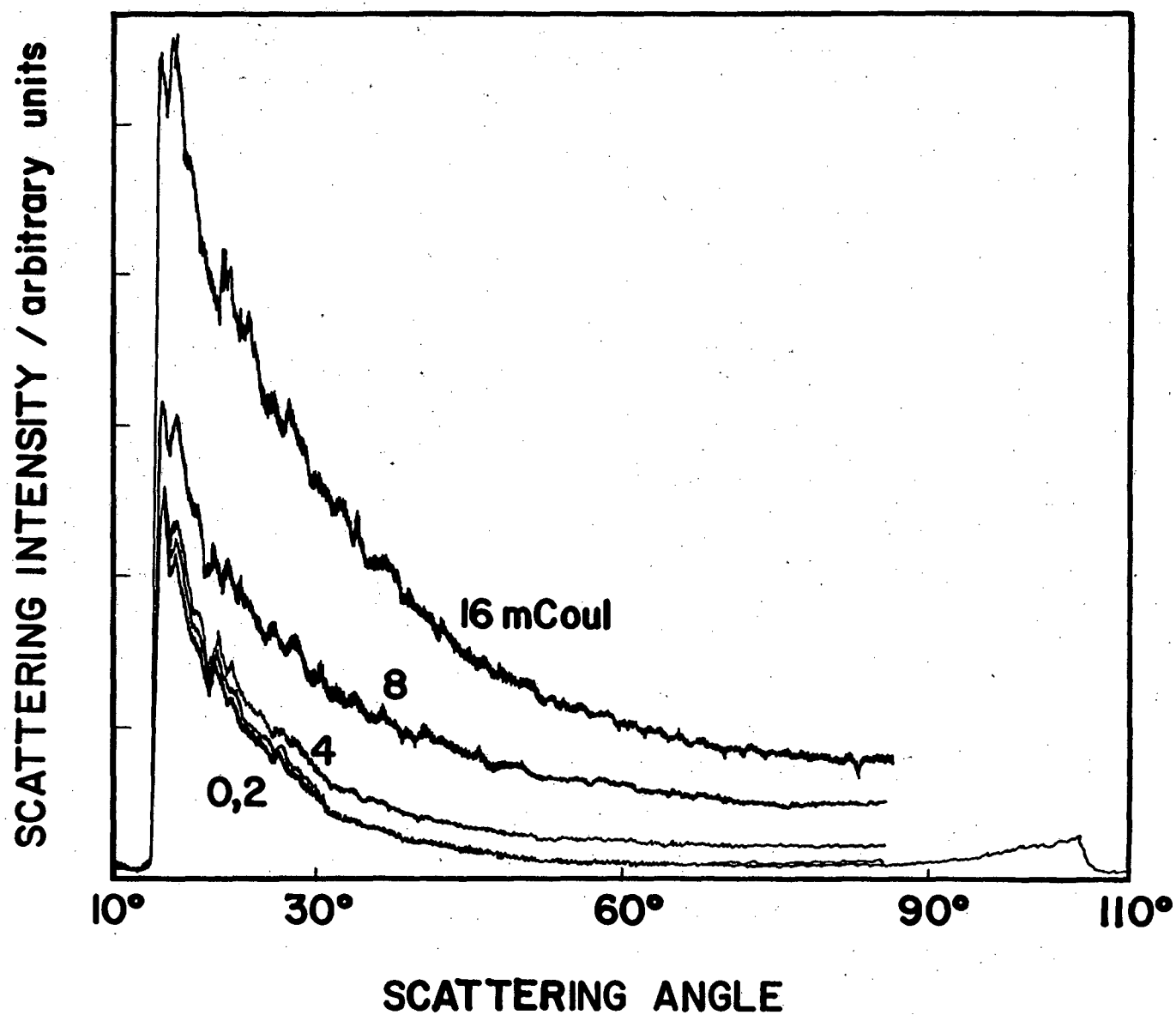

XBL 817-10536

Fig. 2

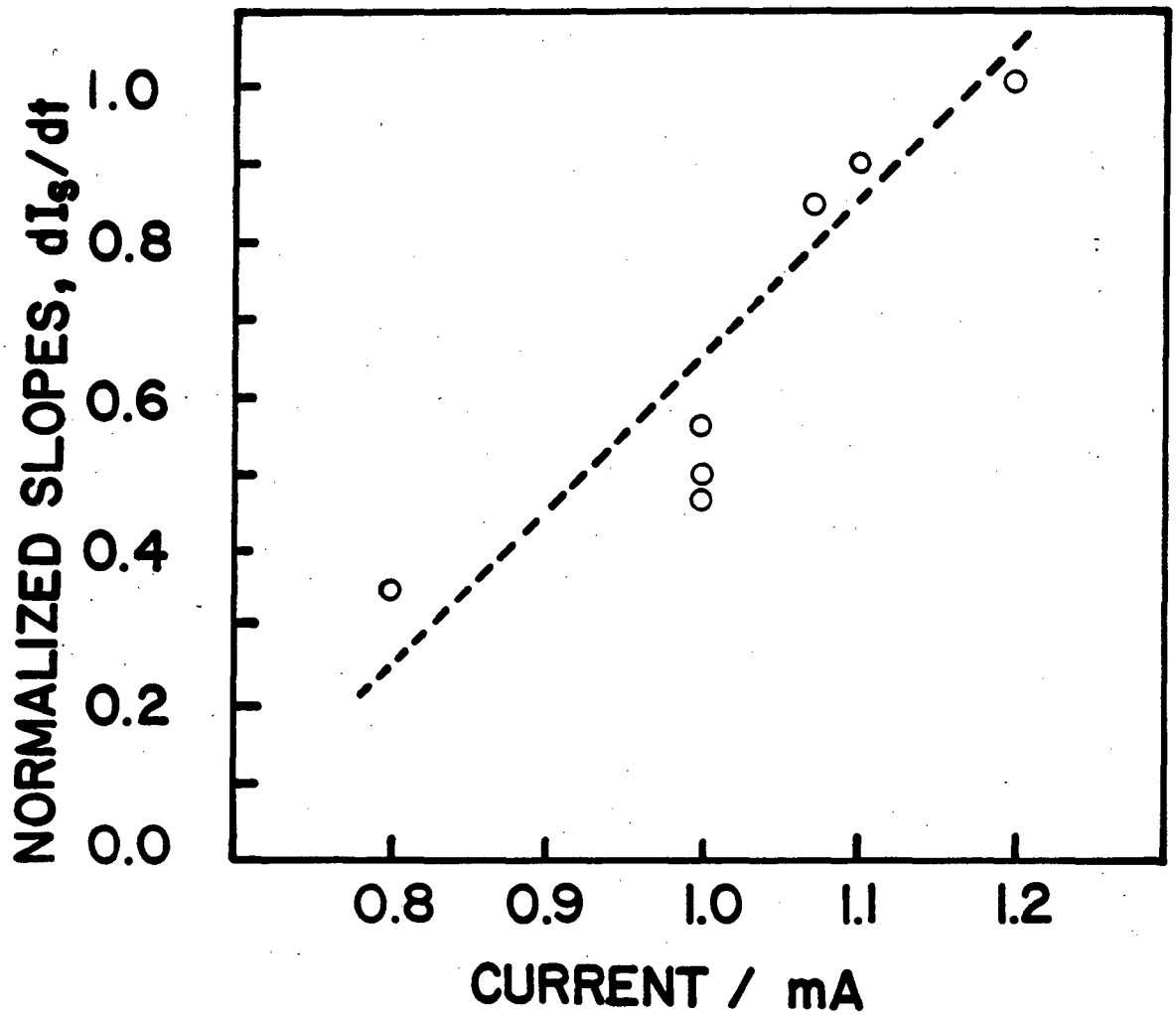

XBL 817-10537

Fig. 3

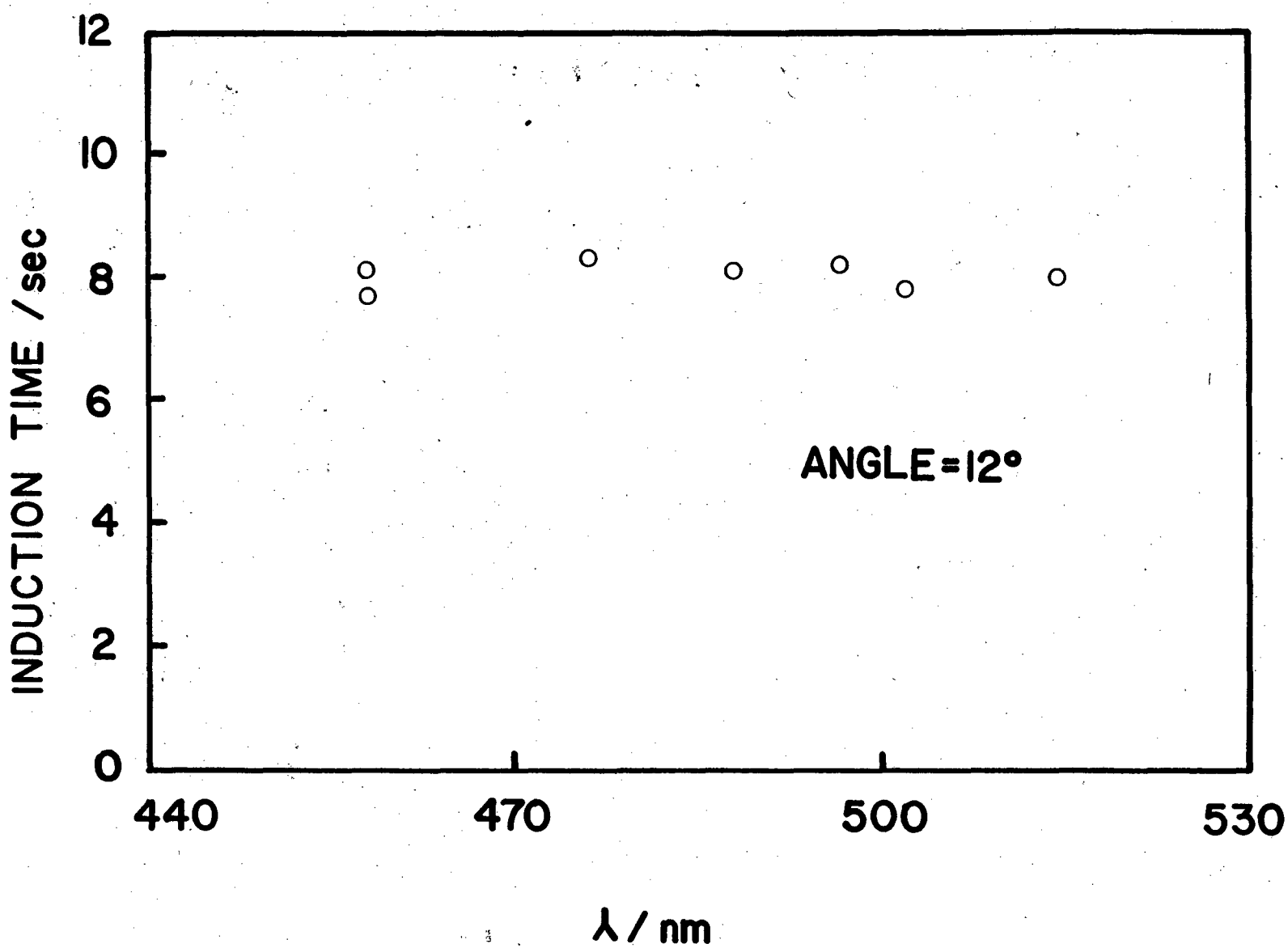

XBL 817-10538

Fig. 4

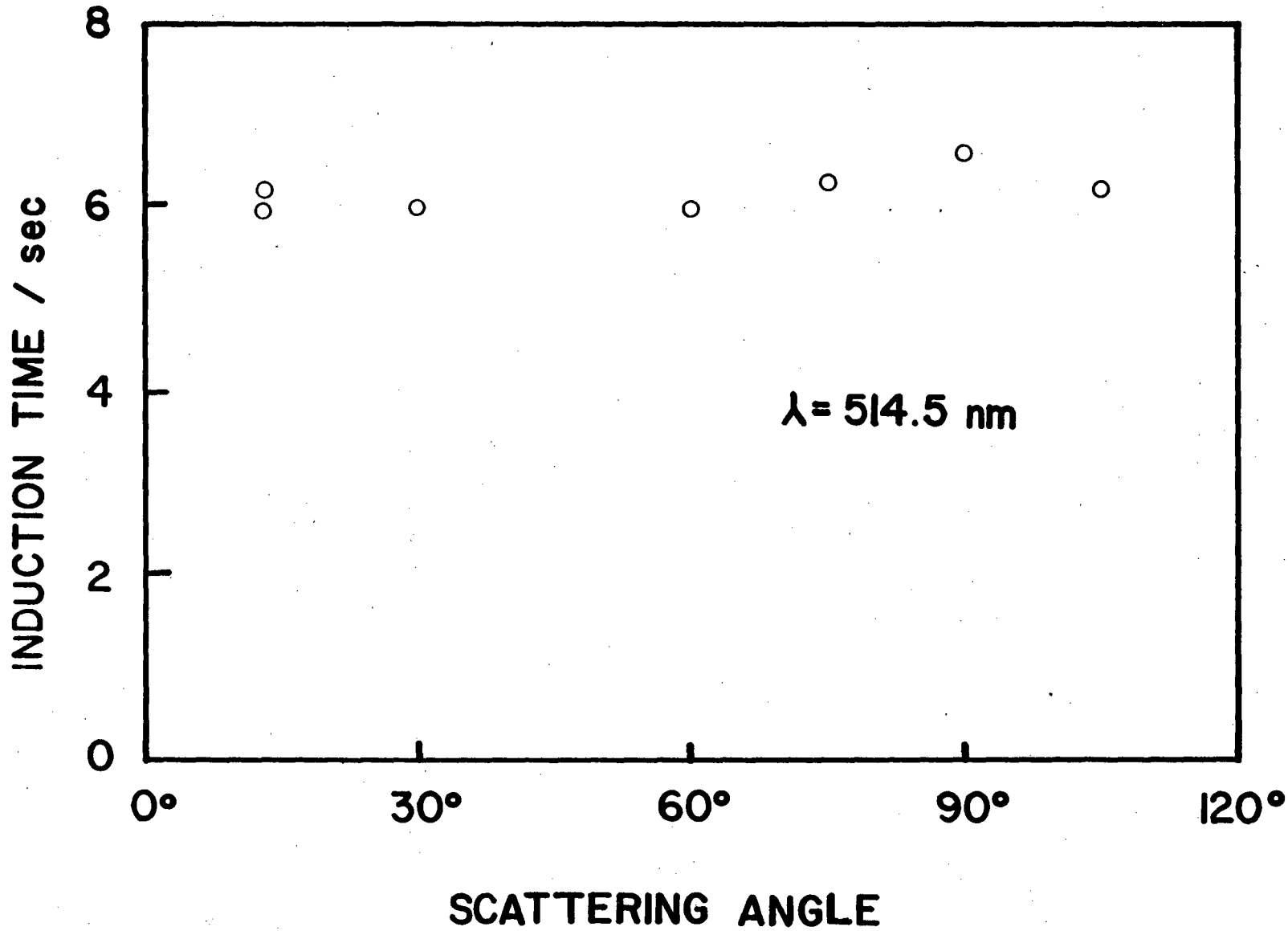

XBL 817-10539

Fig. 5

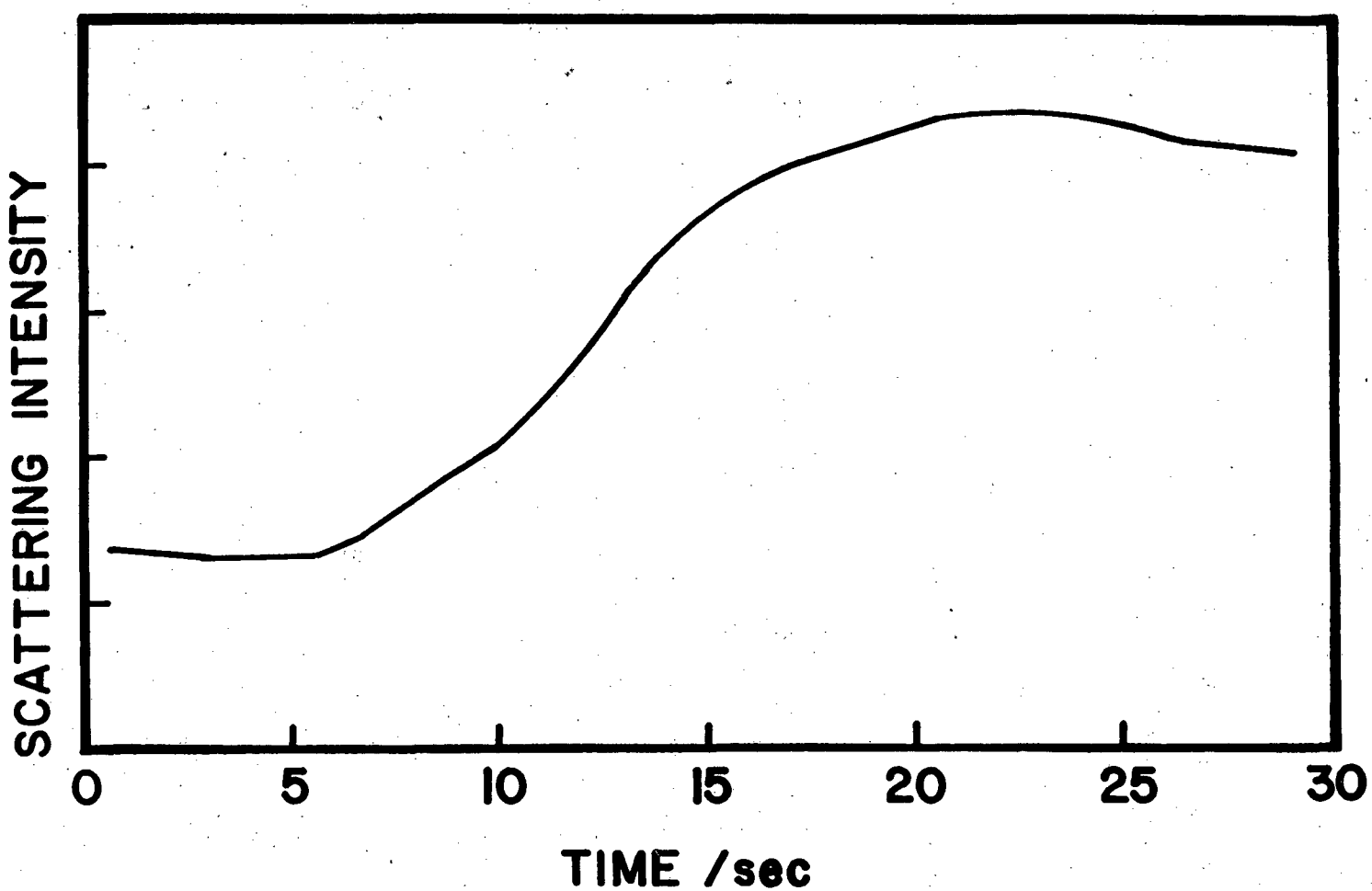

XBL 817-10531

Fig. 6

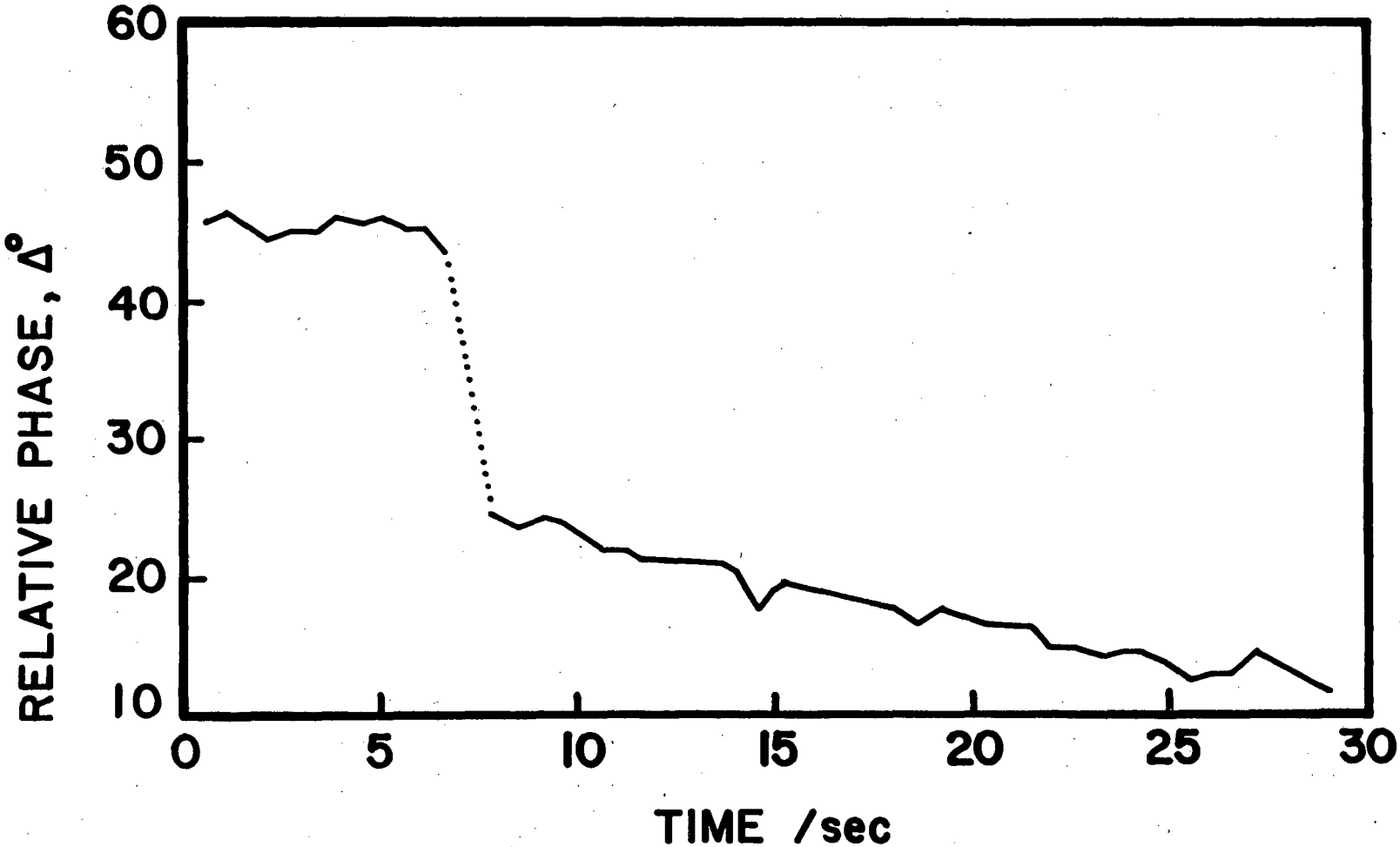

XBL 817-10533

Fig. 7

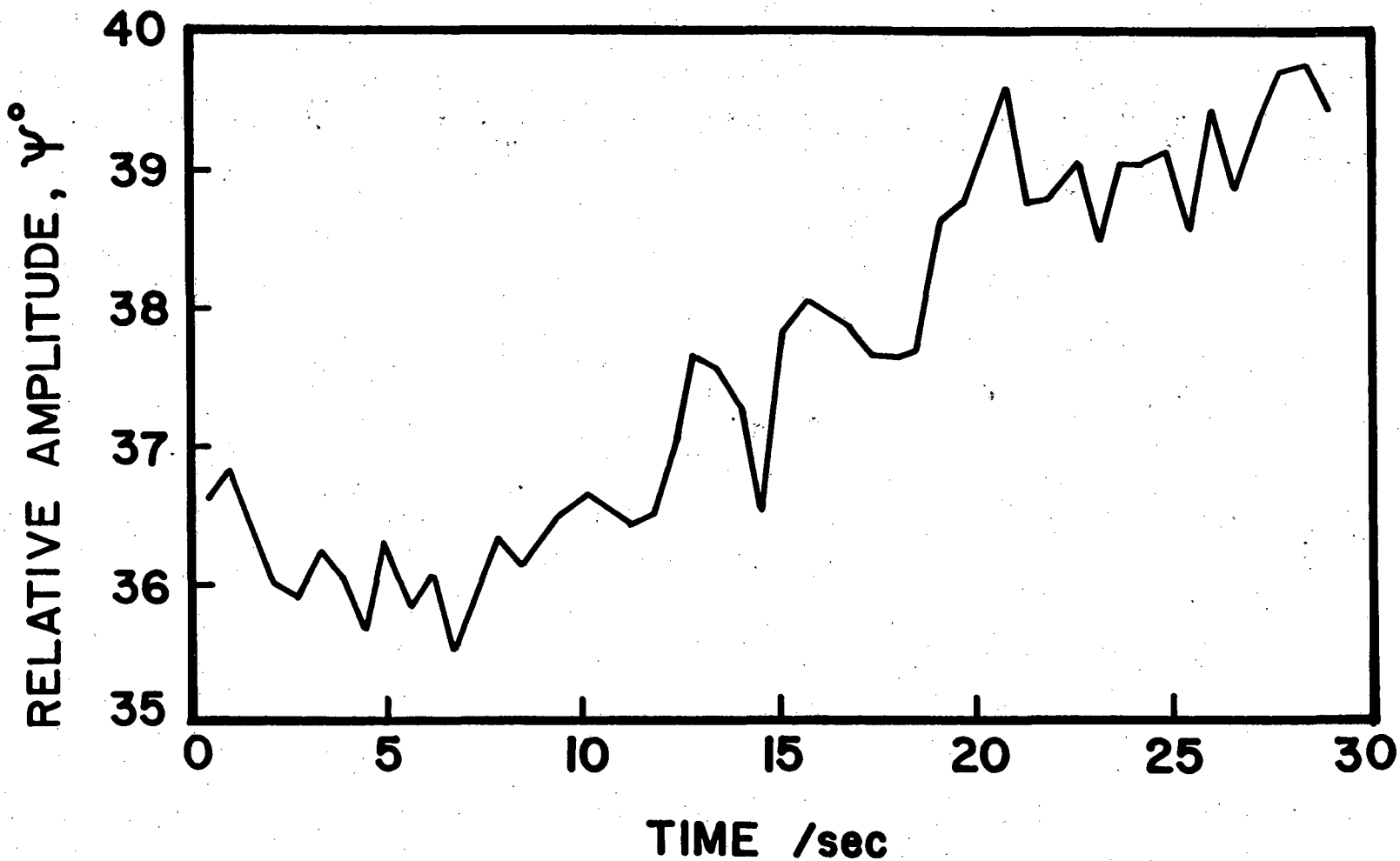

XBL 817-10532

Fig. 8

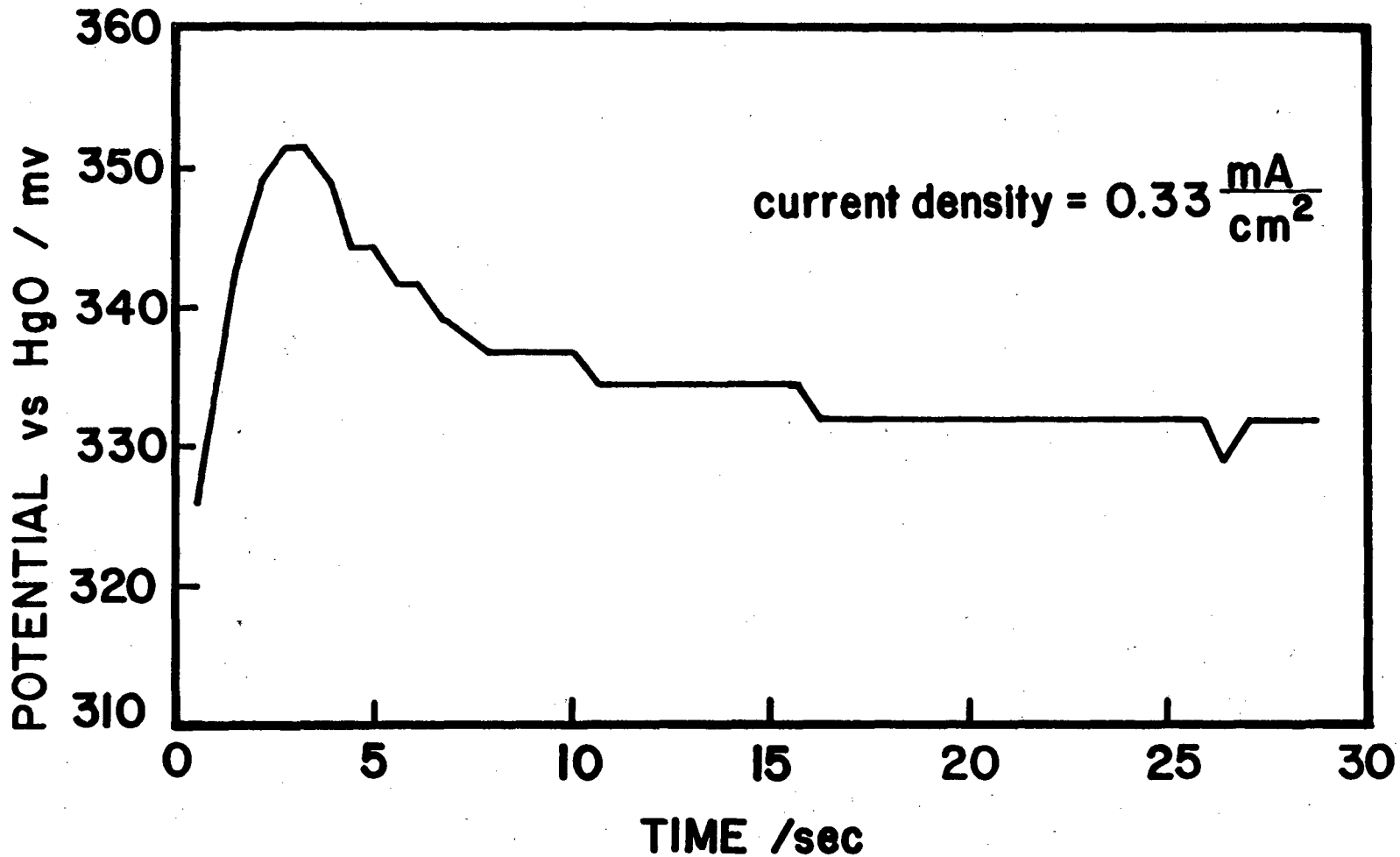

XBL 817-10534

Fig. 9

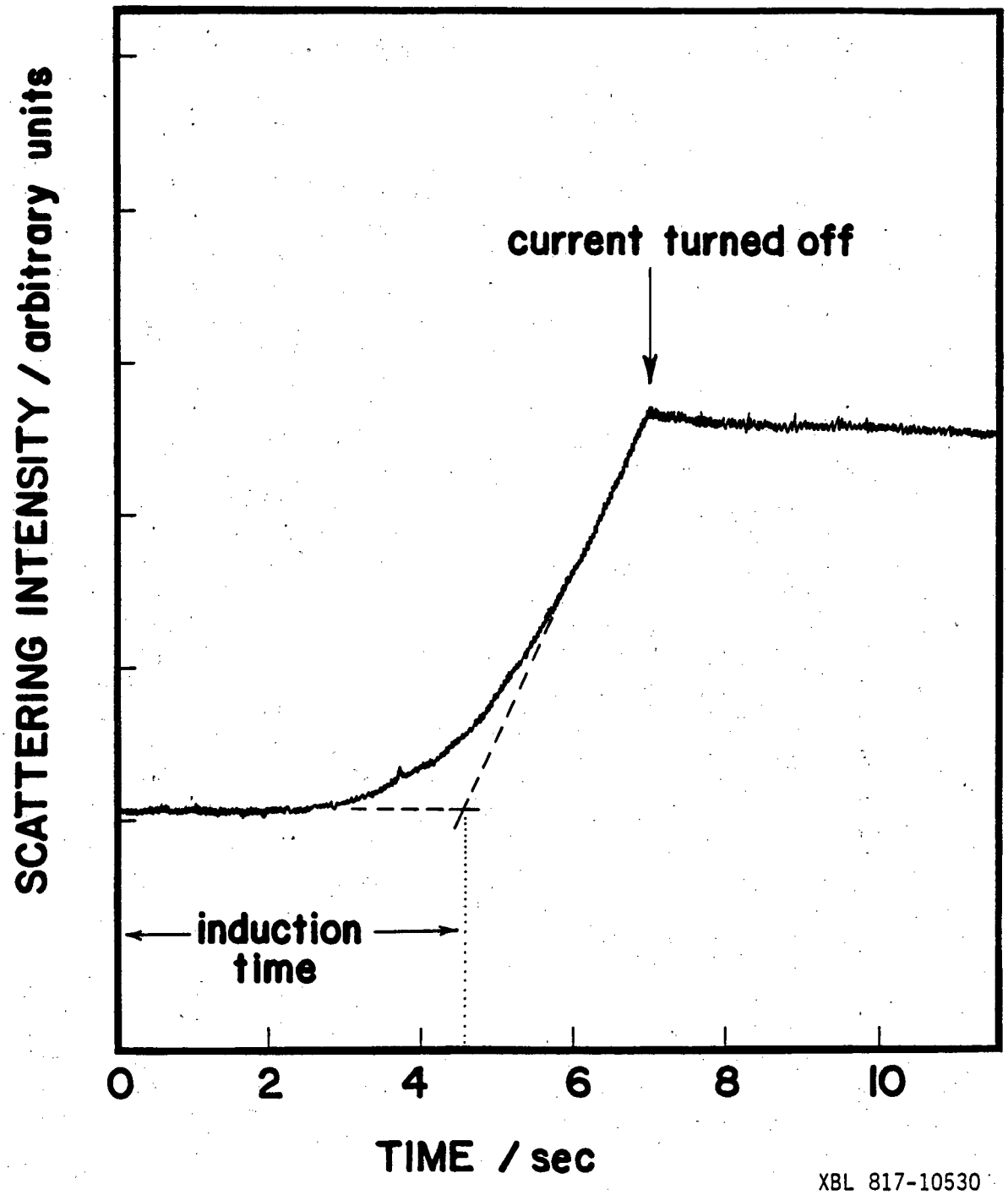
current turned off
SCATTERING INTENSITY / arbitrary units
induction time
0
2
4
6
8
10
TIME / sec
XBL 817-10530

Fig. 10

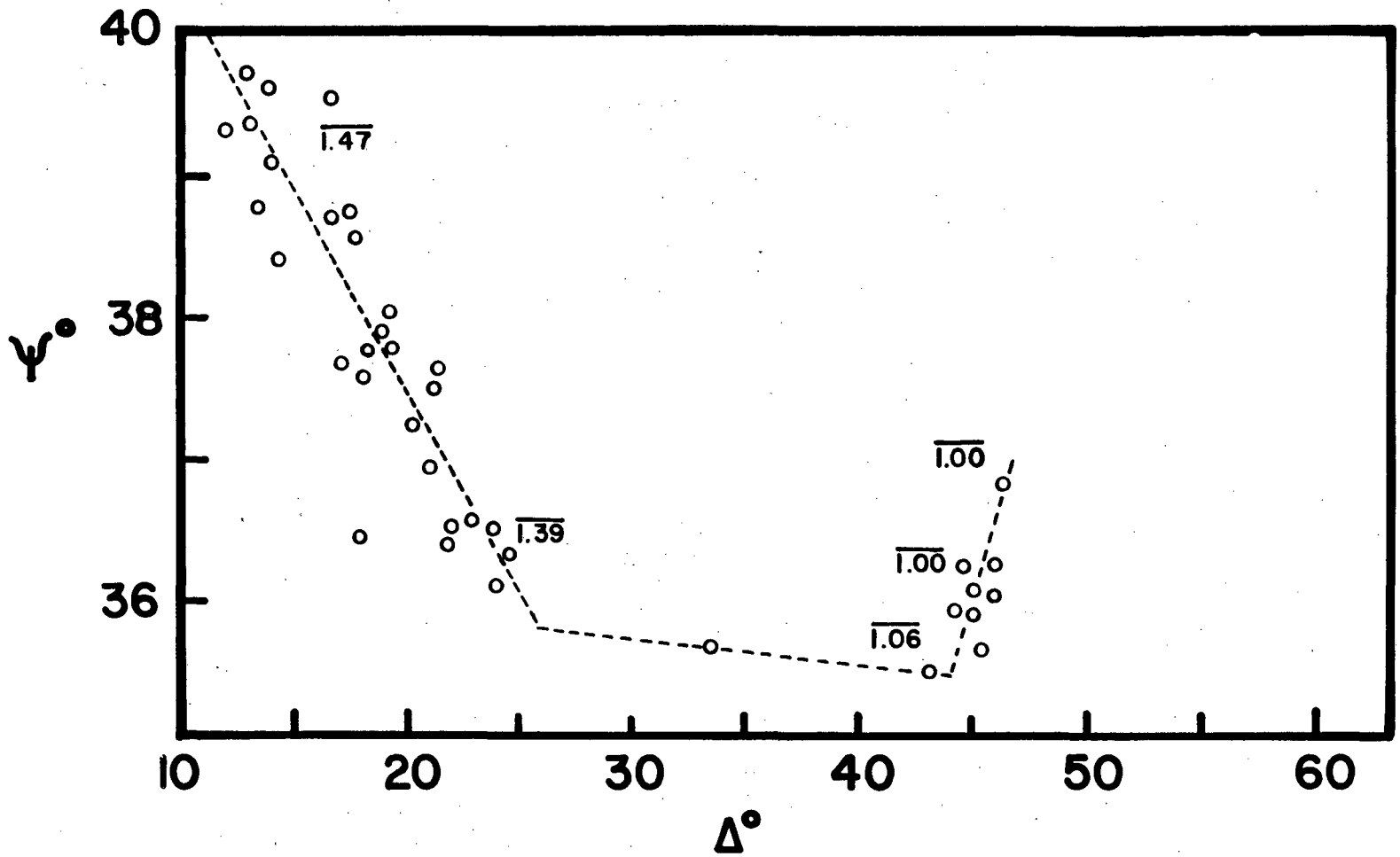

XBL 817-10535

Fig. 11

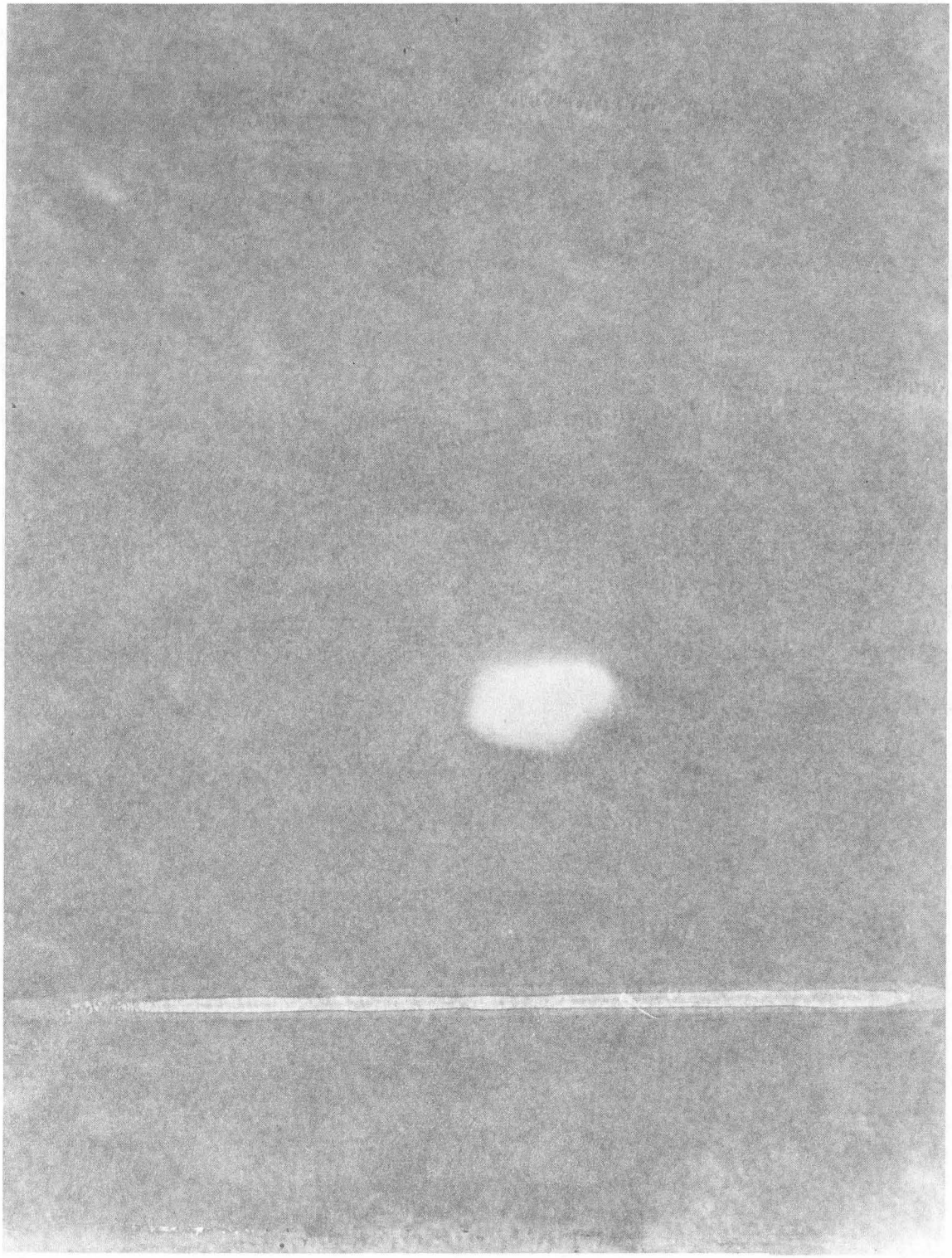

XBB810-10134

Fig. 12

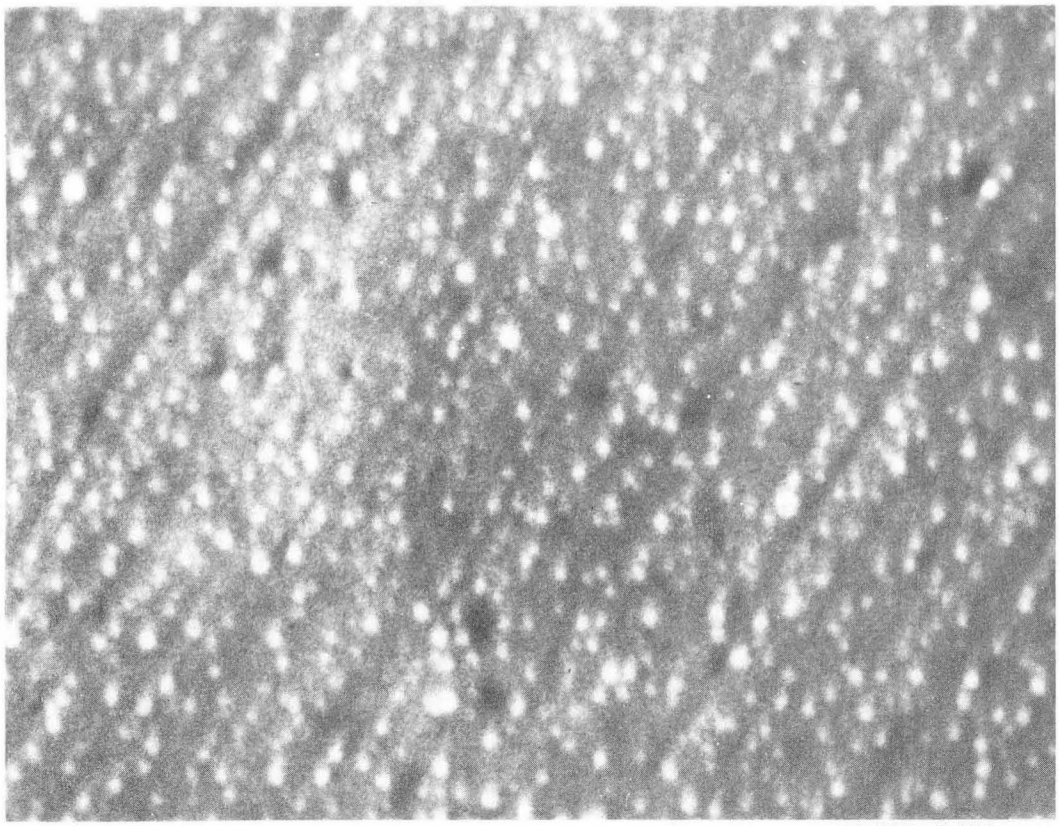

XBB817-5953

Fig. 13

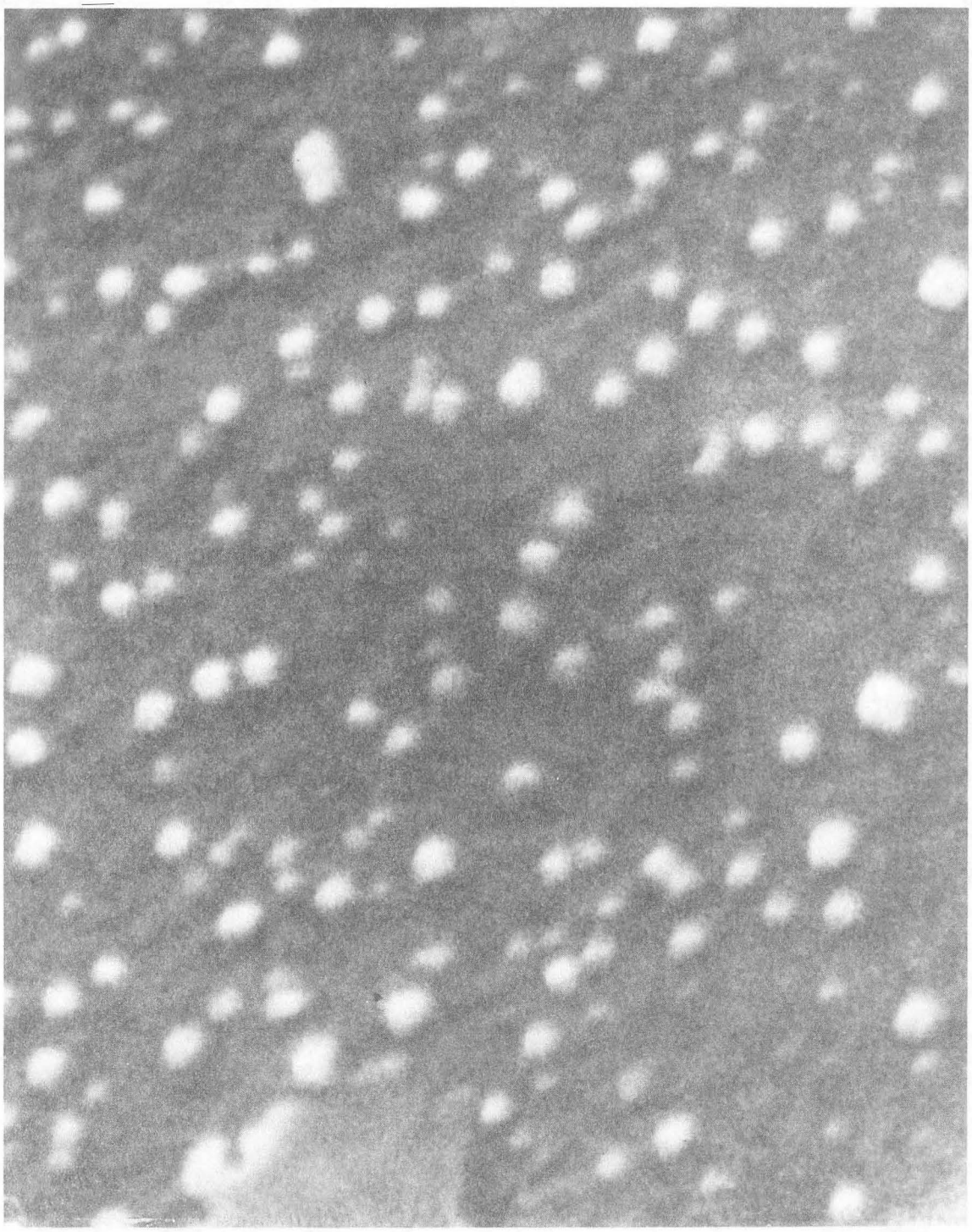

XBB810-10138

Fig. 14(a.)

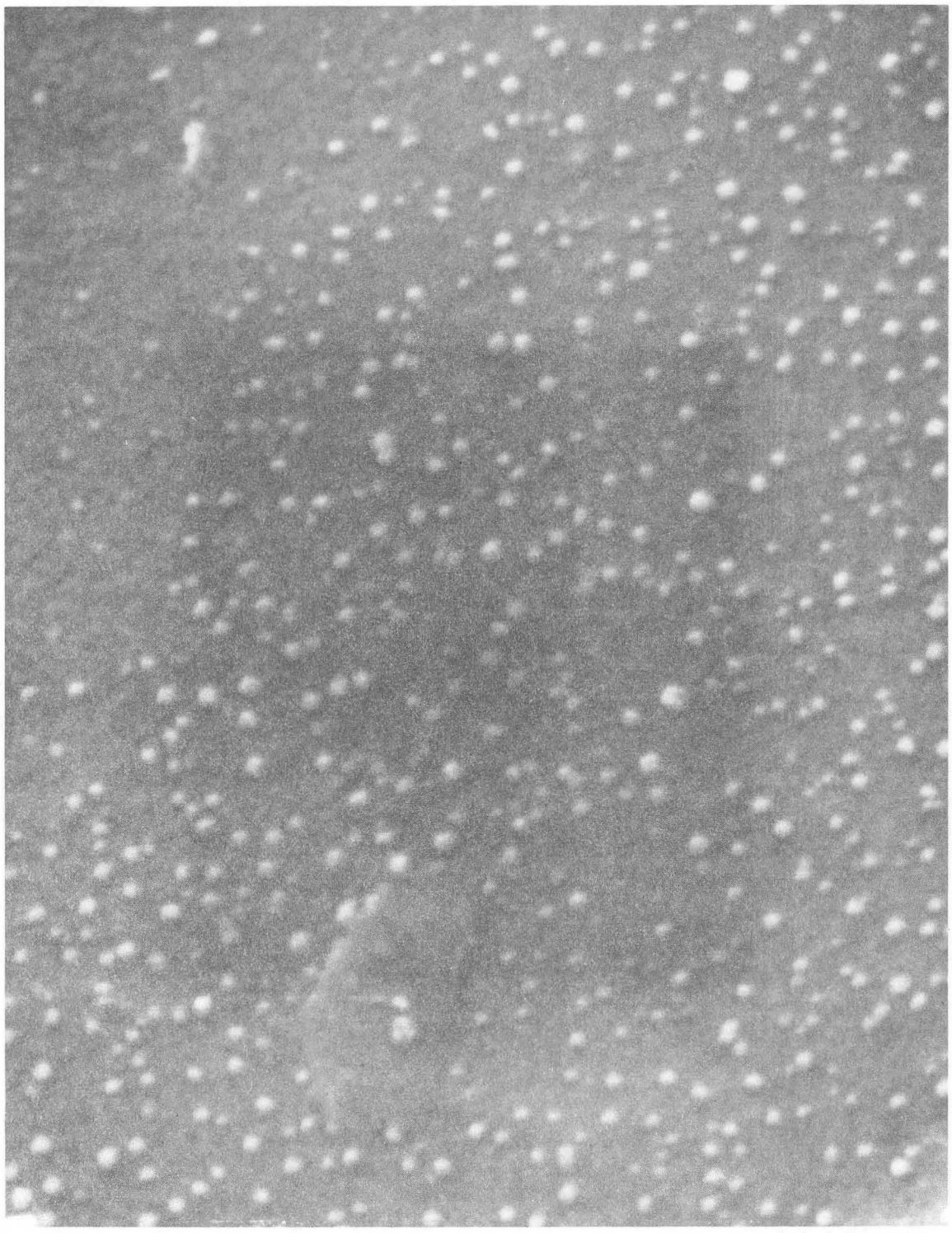

XBB810-10136

Fig. 14(b.)

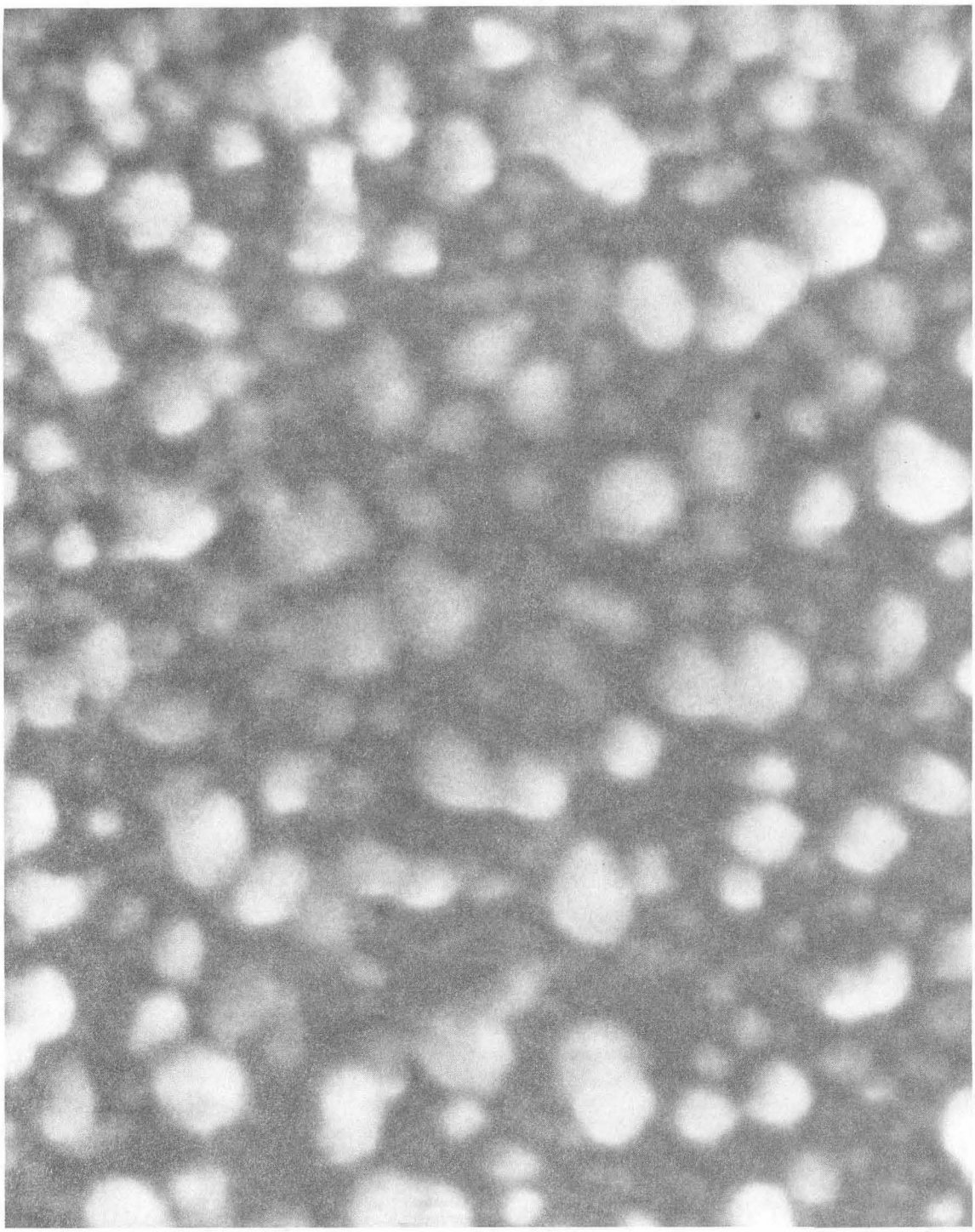

XBB810-10137

Fig. 15(a.)

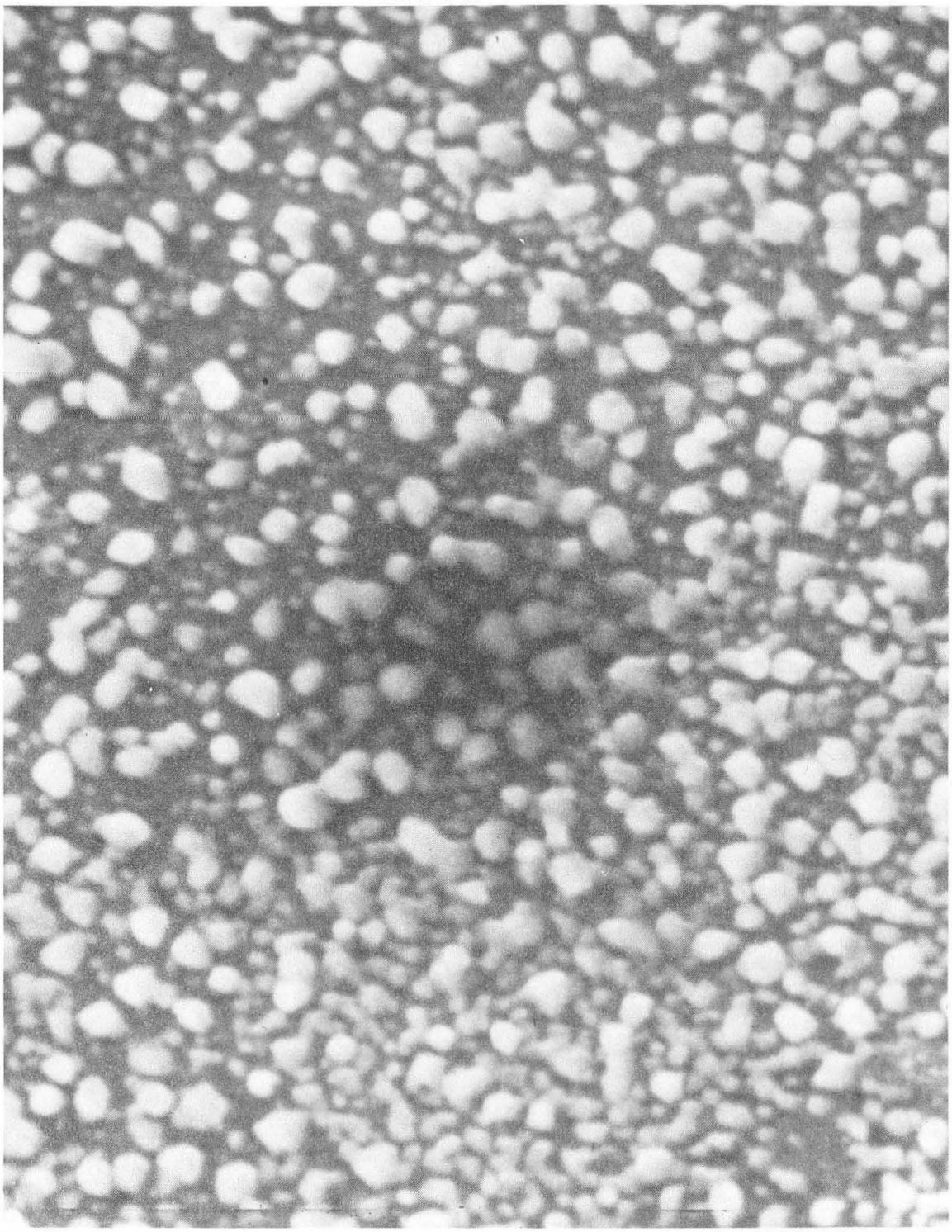

XBB810-10135

Fig. 15(b.)

APPENDIX I

```
      PROGRAM CSFIT
      COMMON/FLMDAT/TN1,TNF,TNKF,TNS,TNKS,WL,PHI1,T,DELC,PSIC
      COMMON/THETA/THETA
      COMMON/ARRAY/X(511),Y(235),INDEX
      COMPLEX TN2,TN3,CPHI2,CPHI3,R1S,R1P,R2S,R2P,Z,RS,RP,RHO
      COMPLEX RSX,RPX,RSY,RPY
      REAL MTHETA,MTHICK
   97 FORMAT(I3)
   98 FORMAT(A1)
   99 FORMAT(F10.4)
      TYPE 1
    1 FORMAT(/,'$ PHI = ')
      ACCEPT 99,PHI1
      TYPE 2
    2 FORMAT(/,'$ WL  = ')
      ACCEPT 99,WL
      TYPE 10
   10 FORMAT(/,'$ N0 = ')
      ACCEPT 99,TN1
      TYPE 20
   20 FORMAT(/,'$ NF = ')
      ACCEPT 99,TNF
      TYPE 25
   25 FORMAT(/,'$ KF = ')
      ACCEPT 99,TNKF
      TYPE 30
   30 FORMAT(/,'$ NS = ')
      ACCEPT 99,TNS
      TYPE 35
   35 FORMAT(/,'$ KS = ')
      ACCEPT 99,TNKS
  100 CONTINUE
      TYPE 40
   40 FORMAT(/,'$ DELM = ')
      ACCEPT 99,DELM
      TYPE 45
   45 FORMAT(/,'$ PSIM = ')
      ACCEPT 99,PSIM
      TYPE 50
   50 FORMAT(/,'$ LOWER THICKNESS LIMIT = ')
      ACCEPT 99,TL
      TYPE 55
   55 FORMAT(/,'$ UPPER THICKNESS LIMIT = ')
      ACCEPT 99,TU
```

APPENDIX I (con't.)

```
      TYPE 60
   60 FORMAT(/,'$ INDEX = ')
      ACCEPT 97,INDEX
      ERRMIN=1.E06
      DT=(TU-TL)/INDEX
      DO 210 I=1,INDEX
      T=TL+(I-1)*DT
      ERRFIT=1.0E06
      DO 200 J=1,100
      THETA=(J-1)*0.01
      CALL FILM02
      ERROR=SQRT((DELM-DELC)**2+(PSIM-PSIC)**2)
      IF(ERROR.GT.ERRFIT)GOTO 200
      ERRFIT=ERROR
      DELFIT=DELC
      PSIFIT=PSIC
      FTHETA=THETA
  200 CONTINUE
      X(I)=T
      Y(I)=ERRFIT
      IF(ERRFIT.GT.ERRMIN)GOTO 210
      ERRMIN=ERRFIT
      DELMIN=DELFIT
      PSIMIN=PSIFIT
      MTHETA=FTHETA
      MTHICK=T
  210 TYPE 220,ERRFIT,DELFIT,PSIFIT,FTHETA,T
  220 FORMAT(5(2X,F10.4))
      PRINT 250,PHI1,WL,TN1,TNF,TNKF,TNS,TNKS,DELM,DELMIN,PSIM,PSIMIN
     C,ERRMIN,MTHICK,MTHETA
  250 FORMAT(//,' ANGLE OF INCIDENCE = ',F3.0,5X,'WAVELENGTH = ',F5.0,
     C       //,' AMBIENT   REFRACTIVE INDEX = ',F5.2,
     C        /,' FILM      REFRACTIVE INDEX = ',F5.2,' - ',F5.2,'I',
     C        /,' SUBSTRATE REFRACTIVE INDEX = ',F5.2,' - ',F5.2,'I',
     C       //,' MEASURED VALUE OF DELTA    = ',F7.2,' CALCULATED....'
     C,F7.2,
     C        /,' MEASURED VALUE OF PSI      = ',F7.2,' CALCULATED....'
     C,F7.2,
     C        /,' ERROR BY SUM OF SQUARES    = ',F7.2,
     C        /,' CORRESPONDING THICKNESS    = ',F6.0,
     C        /,' APPARANT SURFACE COVERAGE  = ',F8.4)
      CALL PLOT
      TYPE 300
  300 FORMAT(/,'$ MORE CALCULATIONS? ')
      ACCEPT 98,ANSWER
      IF(ANSWER.EQ.1HY)GOTO 100
      STOP
      END
```

This program finds the apparent surface coverage, θ_C, giving the minimum sum-of-squares for incremented values of the film thickness T_C. The program is completely user prompted; i.e., the user is instructed by the CRT on the program's required input. The theoretical basis for this program is the coherent superposition model.

APPENDIX II

```
      PROGRAM CSPLOT
      COMMON/FLMDAT/TN1,TNF,TNKF,TNS,TNKS,WL,PHI1,T,DELC,PSIC
      COMMON/THETA/THETA
      COMMON/ARRAY/X(511),Y(235),INDEX
      COMPLEX TN2,TN3,CPHI2,CPHI3,R1S,R1P,R2S,R2P,Z,RS,RP,RHO
      COMPLEX RSX,RPX,RSY,RPY
   97 FORMAT(I3)
   98 FORMAT(A1)
   99 FORMAT(F10.4)
      TYPE 1
    1 FORMAT(/,'$ PHI = ')
      ACCEPT 99,PHI1
      TYPE 2
    2 FORMAT(/,'$ WL  = ')
      ACCEPT 99,WL
      TYPE 10
   10 FORMAT(/,'$ N0 = ')
      ACCEPT 99,TN1
      TYPE 20
   20 FORMAT(/,'$ NF = ')
      ACCEPT 99,TNF
      TYPE 25
   25 FORMAT(/,'$ KF = ')
      ACCEPT 99,TNKF
      TYPE 30
   30 FORMAT(/,'$ NS = ')
      ACCEPT 99,TNS
      TYPE 35
   35 FORMAT(/,'$ KS = ')
      ACCEPT 99,TNKS
      TYPE 40
   40 FORMAT(/,'$ DELM = ')
      ACCEPT 99,DELM
      TYPE 45
   45 FORMAT(/,'$ PSIM = ')
      ACCEPT 99,PSIM
  100 CONTINUE
      TYPE 50
   50 FORMAT(/,'$ THICKNESS = ')
      ACCEPT 99,T
```

APPENDIX II (con't.)

```
      TYPE 55
   55 FORMAT(/,'$ INDEX = ')
      ACCEPT 97,INDEX
      THETA=0.
      DTHETA=1./INDEX
      ERRFIT=1.E06
      DO 200 I=1,INDEX
      THETA=THETA+DTHETA
      CALL FILM02
      ERROR=SQRT((DELM-DELC)**2+(PSIM-PSIC)**2)
      TYPE 150,T,THETA,DELC,PSIC,ERROR
  150 FORMAT(5(2X,F10.4))
      X(I)=THETA
      Y(I)=ERROR
      IF(ERROR.GT.ERRFIT)GOTO 200
      ERRFIT=ERROR
      DELFIT=DELC
      PSIFIT=PSIC
      FTHETA=THETA
  200 CONTINUE
      CALL PLOT
      PRINT 250,PHI1,WL,TN1,TNF,TNKF,TNS,TNKS,DELM,DELFIT,PSIM,PSIFIT
     C,ERRFIT,T,FTHETA
  250 FORMAT(//,' ANGLE OF INCIDENCE = ',F3.0,5X,'WAVELENGTH = ',F5.0,
     C       //,' AMBIENT   REFRACTIVE INDEX = ',F5.2,
     C        /,' FILM      REFRACTIVE INDEX = ',F5.2,' - ',F5.2,'I',
     C        /,' SUBSTRATE REFRACTIVE INDEX = ',F5.2,' - ',F5.2,'I',
     C       //,' MEASURED VALUE OF DELTA    = ',F7.2,' CALCULATED....'
     C,F7.2,
     C        /,' MEASURED VALUE OF PSI      = ',F7.2,' CALCULATED....'
     C,F7.2,
     C        /,' ERROR BY SUM OF SQUARES    = ',F7.2,
     C        /,' CORRESPONDING THICKNESS    = ',F6.0,
     C        /,' APPARANT SURFACE COVERAGE  = ',F8.4)
      TYPE 300
  300 FORMAT(/,'$ MORE CALCULATIONS? ')
      ACCEPT 98,ANSWER
      IF(ANSWER.EQ.1HY)GOTO 100
      STOP
      END
```

This program is identical to CSFIT, except that the sum-of-squares surface cross-section for all values of θ_C giving minima at various film thickness are displayed graphically, S vs. T_C.

APPENDIX III

```
      PROGRAM EMAFIT
      COMMON/FLMDAT/TN1,TNF,TNKF,TNS,TNKS,WL,PHI1,T,DELC,PSIC
      COMMON/THETA/THETA
      COMMON/ARRAY/X(511),Y(235),INDEX
      COMPLEX TN2,TN3,CPHI2,CPHI3,R1S,R1P,R2S,R2P,Z,RS,RP,RHO
      COMPLEX RSX,RPX,RSY,RPY
      REAL MTHETA,MTHICK
   97 FORMAT(I3)
   98 FORMAT(A1)
   99 FORMAT(F10.4)
      TYPE 1
    1 FORMAT(/,'$ PHI = ')
      ACCEPT 99,PHI1
      TYPE 2
    2 FORMAT(/,'$ WL  = ')
      ACCEPT 99,WL
      TYPE 10
   10 FORMAT(/,'$ N0 = ')
      ACCEPT 99,TN1
      TYPE 20
   20 FORMAT(/,'$ NF = ')
      ACCEPT 99,TNF
      TNF0=TNF
      TYPE 25
   25 FORMAT(/,'$ KF = ')
      ACCEPT 99,TNKF
      TNKF0=TNKF
      TYPE 30
   30 FORMAT(/,'$ NS = ')
      ACCEPT 99,TNS
      TYPE 35
   35 FORMAT(/,'$ KS = ')
      ACCEPT 99,TNKS
  100 CONTINUE
      TYPE 40
   40 FORMAT(/,'$ DELM = ')
      ACCEPT 99,DELM
      TYPE 45
   45 FORMAT(/,'$ PSIM = ')
      ACCEPT 99,PSIM
      TYPE 50
   50 FORMAT(/,'$ LOWER THICKNESS LIMIT = ')
      ACCEPT 99,TL
      TYPE 55
   55 FORMAT(/,'$ UPPER THICKNESS LIMIT = ')
      ACCEPT 99,TU
```

APPENDIX III (con't.)

```
      TYPE 60
   60 FORMAT(/,'$ INDEX = ')
      ACCEPT 97,INDEX
      ERRMIN=1.E06
      DT=(TU-TL)/INDEX
      DO 210 I=1,INDEX
      T=TL+(I-1)*DT
      ERRFIT=1.0E06
      DO 200 J=1,100
      THETA=(J-1)*0.01
      TNF=TNF0
      TNKF=TNKF0
      CALL EMA
      CALL FILM
      ERROR=SQRT((DELM-DELC)**2+(PSIM-PSIC)**2)
      IF(ERROR.GT.ERRFIT)GOTO 200
      ERRFIT=ERROR
      DELFIT=DELC
      PSIFIT=PSIC
      FTHETA=THETA
  200 CONTINUE
      X(I)=T
      Y(I)=ERRFIT
      IF(ERRFIT.GT.ERRMIN)GOTO 210
      ERRMIN=ERRFIT
      DELMIN=DELFIT
      PSIMIN=PSIFIT
      MTHETA=FTHETA
      MTHICK=T
```

APPENDIX III (con't.)

```
210 TYPE 220,ERRFIT,DELFIT,PSIFIT,FTHETA,T
220 FORMAT(5(2X,F10.4))
    PRINT 250,PHI1,WL,TN1,TNF,TNKF,TNS,TNKS,DELM,DELMIN,PSIM,PSIMIN
   C,ERRMIN,MTHICK,MTHETA
250 FORMAT(//,' ANGLE OF INCIDENCE = ',F3.0,5X,'WAVELENGTH = ',F5.0,
   C       //,' AMBIENT   REFRACTIVE INDEX = ',F5.2,
   C        /,' FILM      REFRACTIVE INDEX = ',F5.2,' - ',F5.2,'I',
   C        /,' SUBSTRATE REFRACTIVE INDEX = ',F5.2,' - ',F5.2,'I',
   C       //,' MEASURED VALUE OF DELTA    = ',F7.2,' CALCULATED....'
   C,F7.2,
   C        /,' MEASURED VALUE OF PSI      = ',F7.2,' CALCULATED....'
   C,F7.2,
   C        /,' ERROR BY SUM OF SQUARES    = ',F7.2,
   C        /,' CORRESPONDING THICKNESS    = ',F6.0,
   C        /,' APPARANT SURFACE COVERAGE  = ',F8.4)
    CALL PLOT
    TYPE 300
300 FORMAT(/,'$ MORE CALCULATIONS? ')
    ACCEPT 98,ANSWER
    IF(ANSWER.EQ.1HY)GOTO 100
    STOP
    END
```

Comparable to CSPLOT, except the theoretical basis of this calculation is the Bruggeman Effective Media Approximation.

APPENDIX IV

```
SUBROUTINE EMA
COMMON/FLMDAT/TN1,TNF,TNKF,TNS,TNKS,WL,PHI1,T,DELC,PSIC
COMMON/THETA/THETA
COMPLEX TN2,TN3,CPHI3,R1S,R1P,R2S,R2P,Z,RS,RP,RHO
COMPLEX E,E1,E2,A,B
E1=CMPLX(TNF,-TNKF)
TNA=TN1
TNAF=0.
E2=CMPLX(TNA,-TNAF)
E1=E1*E1
E2=E2*E2
X1=THETA
X2=1.-THETA
A=0.5*(E1*(X2-2.*X1)+E2*(X1-2.*X2))
B=-0.5*(E1*E2)
E=0.5*(-A+CSQRT(A*A-4.*B))
TN2=CSQRT(E)
TNF=REAL(TN2)
TNKF=-AIMAG(TN2)
RETURN
END
```

This subroutine computes the apparent film complex refractive index using the EMA mixing rule for EMAFIT.

APPENDIX V

```
      SUBROUTINE FILM
C*********************************************************************
C     THIS SUBROUTINE COMPUTES "PSI" AND "DELTA" FOR A SIMPLE HOMO-
C     GENEOUS FILM ON A SUBSTRATE GIVEN (1) THE REFRACTIVE INDICES OF
C     THE SUBSTRATE, FILM, AND INCIDENT MEDIUM; (2) THE FILM THICKNESS;
C     (3) THE WAVELENGTH OF THE SOURCE; AND (4) THE ANGLE OF INCIDENCE.
C*********************************************************************
      COMMON/FLMDAT/TN1,TNF,TNKF,TNS,TNKS,WL,PHI1,T,DELC,PSIC
      COMPLEX TN2,TN3,CPHI2,CPHI3,R1S,R1P,R2S,R2P,Z,RS,RP,RHO
      PHI=0.01745329252*PHI1
      CP=DCOS(PHI)
      SP=DSIN(PHI)
      TN3=CMPLX(TNS,-TNKS)
      CPHI3=CSQRT(1.0-TN1**2*SP**2/(TN3**2))
      TN2=CMPLX(TNF,-TNKF)
      CPHI2=CSQRT(1.0-TN1**2*SP**2/(TN2**2))
      R1S=(TN1*CP-TN2*CPHI2)/(TN1*CP+TN2*CPHI2)
      R1P=-(TN1*CPHI2-TN2*CP)/(TN1*CPHI2+TN2*CP)
      R2S=(TN2*CPHI2-TN3*CPHI3)/(TN2*CPHI2+TN3*CPHI3)
      R2P=-(TN2*CPHI3-TN3*CPHI2)/(TN2*CPHI3+TN3*CPHI2)
      Z=(0.0,1.0)*(4.0*3.1415927*T/WL)*TN2*CPHI2
      RS=(R1S+R2S*CEXP(-Z))/(1.0+R1S*R2S*CEXP(-Z))
      RP=(R1P+R2P*CEXP(-Z))/(1.0+R1P*R2P*CEXP(-Z))
      RHO=RP/RS
      PSIC=DATAN(CABS(RHO))/0.01745329252
      DELC=DATAN2(AIMAG(RHO),REAL(RHO))/0.01745329252
      RETURN
      END
```

This computes ψ and Δ given refractive index and film thickness information. This subroutine is also used by EMAFIT.

APPENDIX VI

```
      SUBROUTINE PLOT
      COMMON/ARRAY/X(511),Y(235),INDEX
      COMMON/LIMITS/ILIMX,ILIMY,IGRIDX,IGRIDY,IDELX,IDELY
      COMMON/STATUS/ISTAT(16)
      XLO=X(1)
      XHI=X(1)
      YLO=Y(1)
      YHI=Y(1)
      DO 10 I=2,INDEX
      IF(XLO.GT.X(I))XLO=X(I)
      IF(XHI.LT.X(I))XHI=X(I)
      IF(YLO.GT.Y(I))YLO=Y(I)
      IF(YHI.LT.Y(I))YHI=Y(I)
   10 CONTINUE
      TYPE 1000,XLO,XHI,YLO,YHI
 1000 FORMAT(/,5X,'XLO = ',E14.6,5X,'XHI = ',E14.6,
     1       /,5X,'YLO = ',E14.6,5X,'YHI = ',E14.6)
   20 TYPE 1001
 1001 FORMAT(/,'$ DO YOU WANT TO CHANGE THESE(Y/N)? ')
      ACCEPT 1002,IF1
 1002 FORMAT(A1)
      IF(IF1.NE.1HY.AND.IF1.NE.1HN)GOTO 20
      IF(IF1.EQ.1HN)GOTO 30
      TYPE 1003
 1003 FORMAT(/,'$ XLO = ')
      ACCEPT 1004,XLO
 1004 FORMAT(F10.3)
      TYPE 1005
 1005 FORMAT(/,'$ XHI = ')
      ACCEPT 1004,XHI
      TYPE 1006
 1006 FORMAT(/,'$ YLO = ')
      ACCEPT 1004,YLO
      TYPE 1007
 1007 FORMAT(/,'$ YHI = ')
      ACCEPT 1004,YHI
   30 CONTINUE
      DO 40 I=1,INDEX
      X(I)=(X(I)-XLO)/(XHI-XLO)
   40 Y(I)=(Y(I)-YLO)/(YHI-YLO)
      TYPE 1008
 1008 FORMAT(/,'$ HOW MANY SCALE DIVISIONS DO YOU WANT FOR THE
     1 X-AXIS? ')
      ACCEPT 1009,IGRIDX
 1009 FORMAT(I2)
```

APPENDIX VI (con't)

APPENDIX VI (con't.)

```
      TYPE 1010
 1010 FORMAT(/,'$ HOW MANY SCALE DIVISIONS DO YOU WANT FOR THE
     1 Y-AXIS? ')
      ACCEPT 1009,IGRIDY
      CALL WIPE
      CALL PLOT55(2,2+4+32+64,,ISTAT)
      ILIMX=511
      ILIMY=235
      IDELX=ILIMX/IGRIDX
      IDELY=ILIMY/IGRIDY
      CALL GRID
      M=INDEX/2
      DO 50 I=1,M
      I1=(I-1)*2+1
      MX=X(I1)*ILIMX
      MY=Y(I1)*ILIMY
      CALL PLOT55(1,0,,ISTAT)
      CALL PLOT55(3,MX,MY,ISTAT)
      I2=I*2
      MX=X(I2)*ILIMX
      MY=Y(I2)*ILIMY
      CALL PLOT55(2,0,,ISTAT)
      CALL PLOT55(3,MX,MY,ISTAT)
   50 CONTINUE
      TYPE 1000,XLO,XHI,YLO,YHI
      ACCEPT 1011,IWAIT
 1011 FORMAT(A1)
      CALL WIPE
      RETURN
      END
```

APPENDIX VI (con't.)

```
      SUBROUTINE WIPE
      COMMON/STATUS/ISTAT(16)
      DO 1 I=1,16
    1 ISTAT(I)=0
      CALL PLOT55(13,72,,ISTAT)
      CALL PLOT55(13,74,,ISTAT)
      CALL PLOT55(2,1+512,,ISTAT)
      RETURN
      END

      SUBROUTINE GRID
      COMMON/STATUS/ISTAT(16)
      COMMON/LIMITS/ILIMX,ILIMY,IGRIDX,IGRIDY,IDELX,IDELY
      CALL PLOT55(5,0,1,ISTAT)
      CALL PLOT55(4,1,0,ISTAT)
      DO 1 I=IDELX,ILIMX,IDELX
    1 CALL PLOT55(5,I,1,ISTAT)
      DO 2 I=IDELY,ILIMY,IDELY
    2 CALL PLOT55(4,1,I,ISTAT)
      RETURN
      END
```

This is a plotting routine (general) for the VT-55 graphics terminal making use of the PLOT55 objective file.

COHERENT SUPERPOSITION MODEL: SEM SPECIMEN "C" SUM-OF-SQUARES ERROR vs FILM THICKNESS

ANGLE OF INCIDENCE = 75. WAVELENGTH = 5145.

AMBIENT REFRACTIVE INDEX = 1.34
FILM REFRACTIVE INDEX = 2.17 - 0.28I
SUBSTRATE REFRACTIVE INDEX = 1.01 - 1.58I

MEASURED VALUE OF DELTA = 15.00 CALCULATED.... 15.13
MEASURED VALUE OF PSI = 39.00 CALCULATED.... 38.93
ERROR BY SUM OF SQUARES = 0.15
CORRESPONDING THICKNESS = 1750.
APPARANT SURFACE COVERAGE = 0.7600

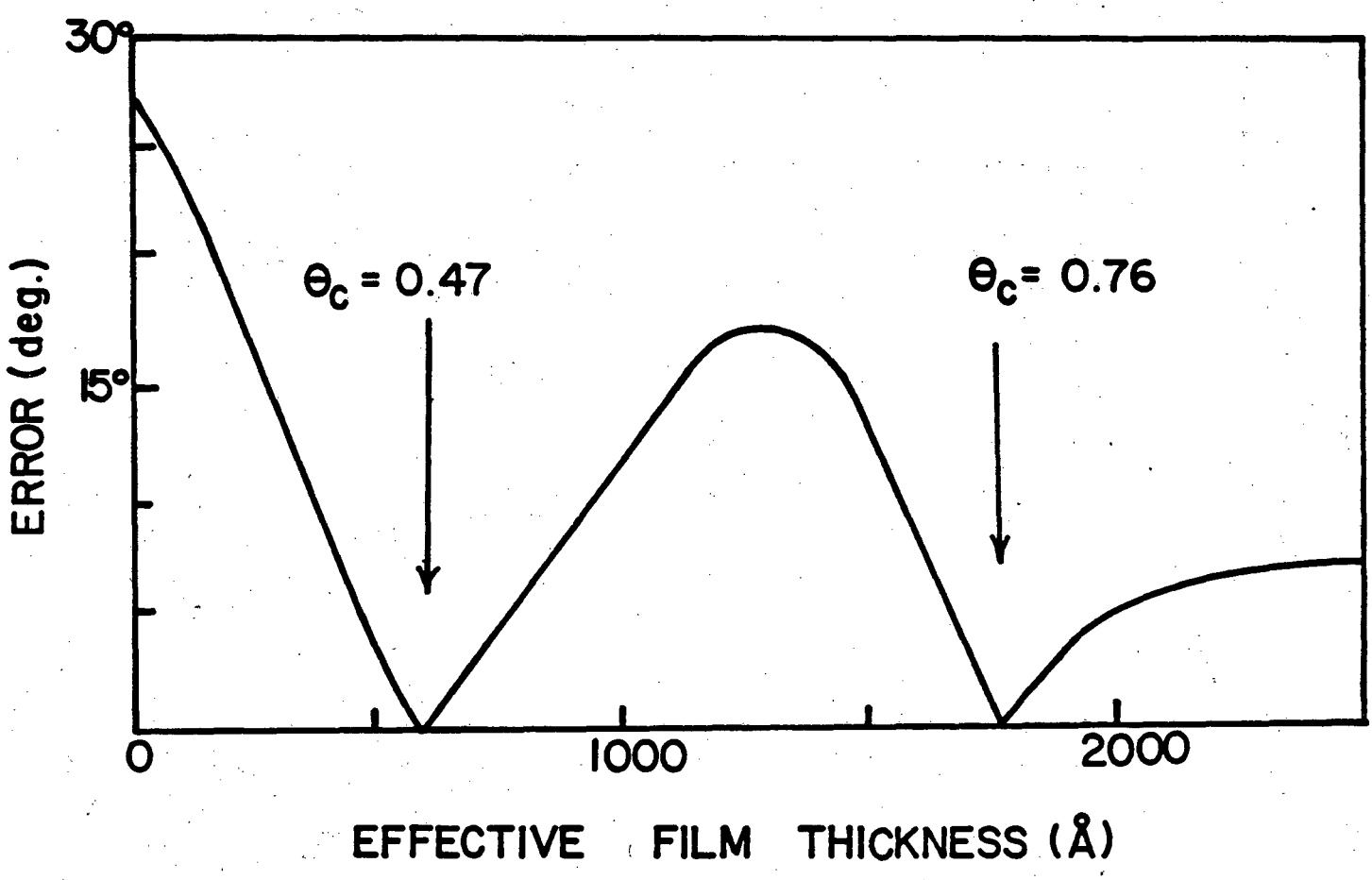

BRUGGEMAN EFFECTIVE MEDIA APPROXIMATION: SEM SPECIMEN "C" SUM-OF-SQUARES ERROR vs FILM THICKNESS

ANGLE OF INCIDENCE = 75. WAVELENGTH = 5145.

AMBIENT REFRACTIVE INDEX = 1.34
FILM REFRACTIVE INDEX = 2.16 - 0.28I
SUBSTRATE REFRACTIVE INDEX = 1.01 - 1.58I

MEASURED VALUE OF DELTA = 15.00 CALCULATED.... 14.83
MEASURED VALUE OF PSI = 39.00 CALCULATED.... 38.88
ERROR BY SUM OF SQUARES = 0.21
CORRESPONDING THICKNESS = 2350.
APPARANT SURFACE COVERAGE = 0.6000

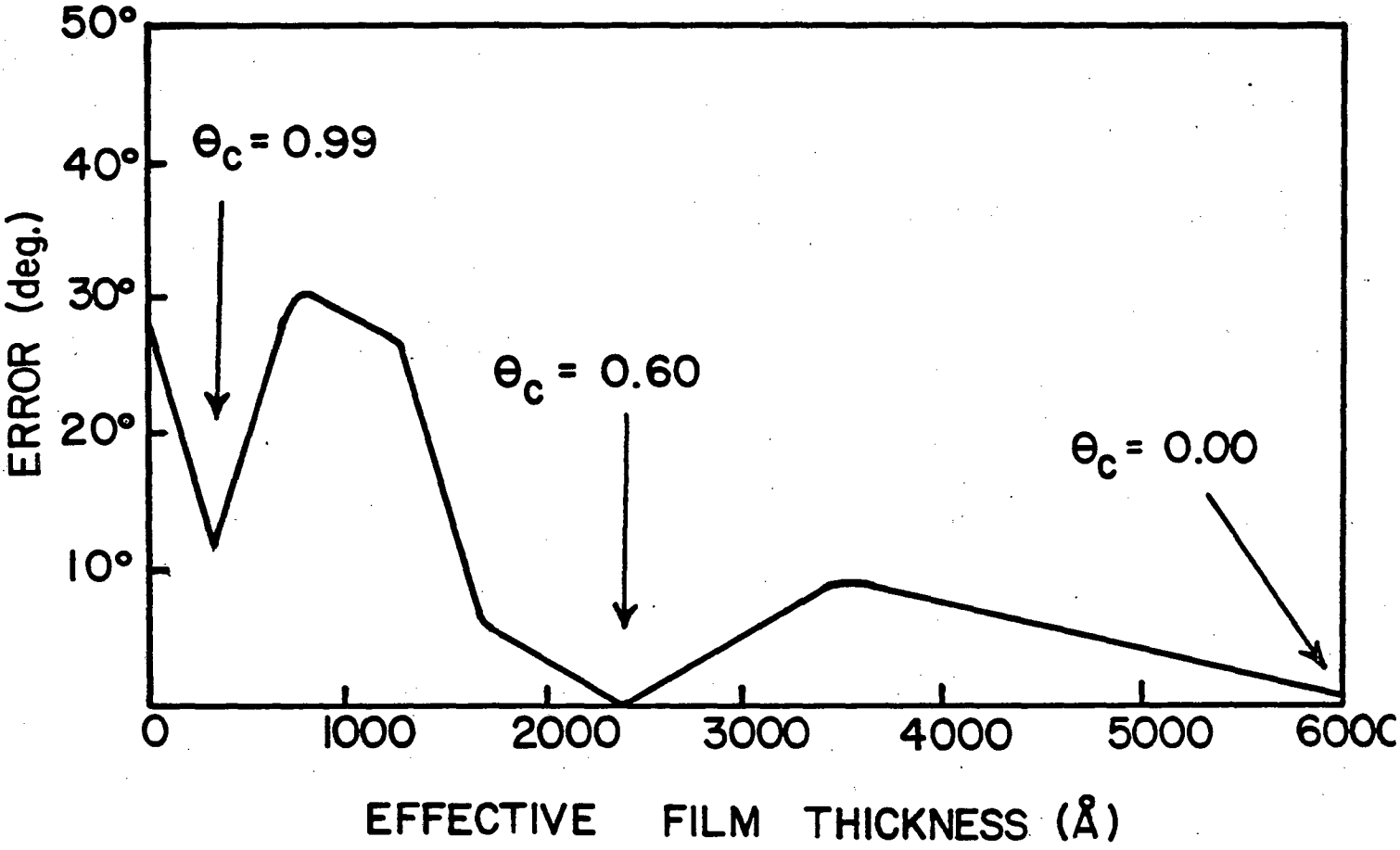

This report was done with support from the Department of Energy. Any conclusions or opinions expressed in this report represent solely those of the author(s) and not necessarily those of The Regents of the University of California, the Lawrence Berkeley Laboratory or the Department of Energy.

Reference to a company or product name does not imply approval or recommendation of the product by the University of California or the U.S. Department of Energy to the exclusion of others that may be suitable.

TECHNICAL INFORMATION DEPARTMENT
LAWRENCE BERKELEY LABORATORY
UNIVERSITY OF CALIFORNIA
BERKELEY, CALIFORNIA 94720